

Measuring Sizes of Marginally Resolved Young Globular Clusters with HST ¹

Matthew N. Carlson² and Jon A. Holtzman³

ABSTRACT

We present a method to derive sizes of marginally resolved star clusters from HST/WFPC2 observations by fitting King models to observations. We describe results on both simulated images and on observations of young compact clusters in NGC 3597 and NGC 1275. From the simulations, we find that we can measure King model concentrations (c) to an accuracy of about a factor of two for all combinations of c and King radius (r_0) of interest if the data have high S/N ($\gtrsim 500$ for the integrated brightness). If the concentration is accurately measured, we can measure the King radius accurately. For lower S/N, marginally resolved King profiles suffer from a degeneracy; different values of the concentration give different r_0 but have comparable reduced χ^2 values. In this case, neither the core radius nor the concentration can be constrained individually, but the half-light radius can be recovered accurately.

In NGC 3597, we can only differentiate between concentrations for the very brightest clusters; these suggest a concentration of ~ 2 . Assuming a concentration of 2 for the rest of the objects, we find an average King radius for the clusters in NGC 3597 of 0.7 pc, while the clusters in NGC 1275 have an average radius of 1.1 pc. These are similar to the average core radii for Galactic globular clusters, 0.92 pc. We find average half-light radii of 5.4 pc and 6.2 pc for the young clusters in NGC 3597 and NGC 1275, respectively, while the average half-light radii of Galactic globulars is 3.4 pc. The spread in the derived radial parameters in each cluster system is comparable to that observed in the Galactic globular cluster system.

Subject headings: galaxies: star clusters

1. Introduction

In the past several years, many observations of young, massive, compact star clusters have been reported in a variety of different galaxies (see *e.g.*, Ashman & Zepf 1998). In many respects,

²1571 Warburton #5, Santa Clara, CA 95050, mcarlson@corsair.com

³Department of Astronomy, New Mexico State University, Dept 4500 Box 30001, Las Cruces, NM 88003, holtz@nmsu.edu

¹Based on observations with the NASA/ESA *Hubble Space Telescope*, obtained at the Space Telescope Science Institute, operated by AURA Inc under contract to NASA

these objects are similar to globular clusters as they would have appeared at a younger age. As such, they may provide clues about the origin of globular cluster systems and the reasons why such systems differ between galaxies of different morphological types.

The range of masses of the young clusters as inferred from colors and population synthesis models are within the range of masses of Galactic globular clusters, if one assumes an IMF that is not deficient in low mass stars. The sizes of the clusters are somewhat more difficult to constrain, given the distances of the galaxies in which many blue cluster systems are found, and it is this problem that we address in this paper.

Measuring structural parameters of young compact clusters is also relevant to determine the degree to which star cluster destruction is important in the evolution of galaxies. The luminosity functions of young cluster systems studied in detail to date differ from those of old globular clusters, as they have an exponentially increasing distribution rather than the log-normal distribution of old globular clusters (*e.g.*, Carlson *et al.* 1998, 1999, Whitmore *et al.* 1999, Zepf *et al.* 1999). As a result, cluster destruction must be very important, and dependent on mass, if the observed young cluster systems are to evolve to look like older systems. The alternative is that the initial mass spectrum of clusters is different in locations today where we are seeing them than it was in the locations where globular clusters formed. Understanding the importance of cluster destruction is also critical to understanding the relative number of cluster vs. field stars formed in a merger, which leads to an understanding of whether the specific frequency of a cluster population can change during an event in which massive star clusters form (*e.g.*, Carlson *et al.* 1999).

To date, observational attempts to constrain the sizes of young globular clusters have been largely made by comparing cluster aperture magnitude differences to stellar and/or model cluster aperture magnitude differences. Holtzman *et al.* (1992) used WFPC1 data to measure the difference between concentric 2 and 4 pixel aperture magnitudes, $m_2 - m_4$, for the young clusters in NGC 1275. From these measurements they concluded that most of the sources were unresolved. Whitmore *et al.* (1993) attempted to determine the half-light radius, r_h , for the clusters in NGC 7252 by comparing the $m_{0.5} - m_3$ to that same difference for model clusters. The models consisted of stellar images broadened by Gaussians. Later work by Holtzman *et al.* (1996) with WFPC2 data used a differential $m_1 - m_2$ value computed by taking the $m_1 - m_2$ for the observed clusters and subtracting the $m_1 - m_2$ for an identically centered model point spread function (PSF). These were compared to the same differential $m_1 - m_2$ calculated for a model PSF broadened by a set of modified Hubble profiles of varying core radii.

Both Gaussians and modified Hubble profiles are rather poor approximations to the surface brightness profiles of globular clusters. In particular, the surface brightness of a Gaussian falls off too rapidly with radius to adequately represent globulars. Galactic globulars are better fit by King models which are based on the model of a cluster of equal mass stars with a truncated Maxwellian distribution of velocities. In a King model (King 1962), the structural properties of globular clusters are represented by three parameters - an amplitude, from the number of stars,

a core radius r_0 , based on the internal dynamics of the system, and a limiting (tidal) radius r_t imposed by the Galactic potential well; often, King models are parameterized by the King radius and the concentration, $c \equiv \log \frac{r_t}{r_0}$.

King models are generally good fits to the density distribution of Galactic globular clusters (e.g., King *et al.* 1968). Later studies extended our knowledge to the structural parameters of a handful of globular clusters in several Local Group galaxies, including the Magellanic Clouds (Chun 1978, Elson & Freeman 1985, Kontizas 1984), M 31 (Crampton *et al.* 1985), and the Fornax dwarf spheroidal (Demers, Kunkel, & Grondin 1990).

With the advent of the Hubble Space Telescope, measurements of globular cluster structural parameters were pushed to NGC 1399 in the Fornax Cluster at 16.9 Mpc (Elson & Schade 1994). They fit King models to 24 old globulars using the Levenberg-Marquardt method and determined r_0 and c for each. The improved resolution of the WFPC2 has allowed the structural parameters of even more distant globular clusters to be studied. Kundu & Whitmore (1998) and Kundu *et al.* (1999) have modeled the light distributions of old globular clusters in the S0 galaxy NGC 3115 and M87 using King models. Their technique uses the cumulative light profile of clusters in several concentric annuli as a way to measure the parameters of the underlying surface brightness profile. For comparison, they constructed numerous template cumulative light profiles for various combinations of centering, position in the field, King radius, and concentration. They determined the King radius and concentration for a given cluster based on the least squares best fit to the cluster from within their grid of template profiles. They noted that they were not able to uniquely fit both the King radius and the concentration simultaneously.

What can we learn from fitting King models to young blue clusters? Perhaps the most important reason to fit King models is to be able to confirm the globular nature of these clusters by comparing their radial parameters to those of known globular clusters, such as those in the Galaxy. Another valuable piece of information comes from the link between cluster concentrations and cluster disruption through mass loss (Weinberg 1993). Clusters with the highest concentration, thus the largest ratios of tidal to King radii, are most prone to disruption by this mechanism. Are the young globulars found in so many galaxies truly stable, or are they going to dissolve in the next 10 Gyr? The concentration of globulars can also give us information about tidal shocking (Surdin 1993). Clusters with low concentrations are subject to disruption by tidal shocks, particularly in the inner parts of galaxies. The tidal radii of globulars are also useful as they can help to place limits on the mass of the host galaxy (Elson & Schade 1994); since the tidal radii of clusters are limited by the gravitational field of the galaxy, they act as direct probes of the galactic mass.

The current paper investigates the measurement of cluster radial parameters by fitting the observed two-dimensional cluster light distributions. The inclusion of data beyond a two or three pixel radius can help differentiate between various models and can better constrain the radial parameters. Section 2 discusses the construction of our models of observed cluster light distributions with the HST/WFPC2, and Section 3 discusses model results on the ability of the fitting procedure

to measure King radii and concentrations as a function of signal-to-noise and angular size.

In Section 4, we apply our method for measuring the radial parameters of young clusters to the cluster systems in NGC 1275 and NGC 3597. The cluster systems in these galaxies were chosen because each has a substantial number of bright clusters for which HST images are available. Each also has a number of bright clusters well away from the central portions of these galaxies where the bright galaxy background makes accurate fitting difficult. The clusters in these galaxies are only marginally resolved. Adopting $H_0 = 75 \text{ km/s/Mpc}$, one pixel of the HST PC frame has a size of ~ 15 parsecs for NGC 1275 ($v = 5264 \text{ km/s}$), while for NGC 3597 ($v = 3485 \text{ km/s}$), one pixel is equivalent to ~ 10 parsecs. So the average core radius of a Galactic globular cluster, ~ 1 pc, corresponds to a small fraction of a pixel. Section 5 discusses the results.

2. Models

To model the observed cluster images, we convolve a WFPC2 Planetary Camera PSF with different functions including a modified Hubble profile, a Gaussian, and a family of King models. These functions provide different models of the underlying stellar surface density distribution.

2.1. PSF

The PSFs used to model the clusters were constructed by optical modeling of the HST mirrors and the WFPC2 camera. The resultant WFPC2 Planetary Camera PSF differs from an ideal diffraction limited image because of the structure of the telescope itself, which leads to diffraction features in the images. Jitter from small changes in the pointing of the telescope broadens the PSF. Slight variations in focus, occurring even within a single exposure, also acts to blur the PSF. The PSF is position-dependent, due to variable aberrations and variation of the pupil function across the PC field of view. These introduce a radial distortion of the PSF causing it to become more elliptical towards the edges of the field. All model PSFs were constructed by a diffraction calculation which modeled these effects; models were computed at 1/4 PC pixel resolution, which corresponds to 0.011 arcsec. Our models also include pixel smearing within the CCD (Burrows *et al.* 1995). This pixel smearing comes from the diffusion of charge in the CCD and is modeled by spreading the counts in a given pixel into neighboring pixels with the following distribution,

$$\begin{array}{ccc} 1\% & 4\% & 1\% \\ 4\% & 80\% & 4\% \\ 1\% & 4\% & 1\% \end{array}$$

with the central pixel retaining 80% of the original counts; neglecting this effect can significantly affect deduced radial parameters. These calculations are very similar to those performed by the

standard TinyTim PSF generator distributed by the Space Telescope Science Institute and the results are nearly identical.

To estimate the effect of PSF variations and uncertainties, we experimented with three different PSF models. The first was our nominal PSF with a typical focus and for an object in the center of the field. The second model was created with a PSF with focus representing the maximum deviation seen in WFPC2 images. The third set of models was appropriate for a PSF at the edge of the field. As discussed below, the effect of using the different PSFs on derived cluster radial parameters was relatively small.

One other possible source of effective degradation of the PSF comes from summing multiple exposures through each filter since frame to frame variations in the pointing can result in a broadened PSF. Attempts to measure this effect in our data sets by correlating shifts in the centroids of individual objects in each of the exposures suggested that the effect on the PSF is very minor for our data sets, so it was not modelled here.

Jitter can also broaden the image, but the effect is usually smaller than that of the poor focus we have assumed in our tests, so we did not include it in our models.

2.2. Functions

To simulate the surface brightness distribution of the star clusters, we used three different functional forms: a Gaussian (Eq. 1), a modified Hubble profile (Eq. 2), and a family of King models. We graphically demonstrate the radial surface brightness distribution of these functions in Figure 1.

$$I = I_0 \exp(r^2/2\sigma^2) \quad (1)$$

$$I = I_0 \left(\frac{1}{1 + (r/r_c)^2} \right) \quad (2)$$

The King model surface brightness distributions were provided by C. Grillmair (private communication) and consist of a series of King models with various concentrations. All models are normalized to have a King radius of 1. The King radius, the tidal radius, and the concentration are related by

$$c \equiv \log(r_t/r_0) \quad (3)$$

Note that the King radius, r_0 , is defined by

$$r_0 \equiv \sqrt{\frac{9\sigma^2}{4\pi G\rho_0}} \quad (4)$$

where σ is the projected velocity dispersion and ρ_0 is the central density. The King radius and core radius (where the surface brightness drops to one half of the central value) of King models are very similar, and the King radius is often simply referred to as the core radius of the King model in the literature.

As can be seen in Figure 1 the Gaussian model is quite different from the modified Hubble profile and King models. The Gaussian falls off much more rapidly than the other models and is a rather poor fit to the extended light profile of a globular cluster; we consider it, however, because it has been used by several authors to model the light distribution of young globulars (Whitmore *et al.* 1993, Whitmore & Schweizer 1995, Schweizer *et al.* 1996). The modified Hubble profile provides a somewhat better fit to the outer regions of a globular cluster surface brightness distribution, and is perhaps the best one parameter fit. Such a model has been used to describe the light distribution of young globulars (Holtzman *et al.* 1992, Holtzman *et al.* 1996, Carlson *et al.* 1998, Carlson *et al.* 1999). While the core radius of the modified Hubble profile is similar to the King radius, it is strictly an empirical fit to the data with no physical significance. As discussed above, however, King models provide the best fits to Galactic globulars and are physically motivated.

Operationally, each of the different functions is constructed at 1/44th of a pixel resolution and normalized to a total flux of 1 count. We chose to construct the functions at this resolution as a compromise between the speed of our fitting procedure and loss of accuracy. Once a functional form for a fit is chosen and constructed, the function is rebinned to quarter pixel resolution to match the resolution of the PSF. The function and the PSF are convolved using a fast Fourier transform, then the output model is centered and rebinned to 1 pixel resolution.

2.3. Fitting Algorithm

Our fits allow for four free parameters - the x and y position of the object, an amplitude, and a radial parameter. For the Gaussian this radial parameter is the full width at half maximum (FWHM), for the modified Hubble profile, it is the core radius, and for the King models, it is the King radius. King models with different concentrations were considered independently and were compared by comparing the quality of the fits, rather than by allowing the concentration to be a free parameter; this avoided the need to be constantly recomputing King models.

The fitting procedure uses the Levenberg-Marquardt method (Marquardt 1963), which is a mixture of the inverse-Hessian method and the method of steepest descents for finding the χ^2 minimum for a model approximation of observational data. After each iteration, the program determines if an acceptable fit has been reached. The fit is accepted if the change in the parameters is less than 0.1% of the previous values for the radial parameter and the amplitude and less than 0.001 pixel

shift in the x and y position of the object and the value of χ^2 has decreased in the last iteration. If the fitting routine doesn't converge in a few dozen iterations, each of the parameters is given a small displacement and the fitting is resumed. This aids in eliminating poor fits. The fit is flagged as suspect if a maximum number of iterations has been reached. If multiple iterations occur without a decrease in χ^2 , the fit is flagged and rejected.

3. Tests of the Models

3.1. Effects of Signal-to-Noise Ratio

To test the effectiveness of the fitting procedure as a function of signal-to-noise, we constructed sets of 100 artificial clusters which included Poisson noise in the signal plus readout noise. Each of these artificial clusters was created using our nominal PSF and was randomly centered within a pixel. We included in these tests three models for the Gaussian function (FWHM = 0.8, 1.4, 2.0 pixels), the modified Hubble profile with three different core radii ($r_c = 0.005, 0.01, 0.03$ pixels), and six King models. For the King models we chose concentrations of 1.0, 1.3, 1.7, 2, 2.3, and 2.95, corresponding to ratios of tidal radii to King radii of 10, 20, 50, 100, 200, and 900, respectively. King model clusters with $c = 2$, which provide the best fit for the brightest of the observed clusters in NGC 3597 (discussed below), were constructed with a set of three different radii, ($r_0 = 0.04, 0.07, 0.15$ pixels). For the other five King models, an average King radius was assumed for each ($r_{0,10} = 0.4, r_{0,20} = 0.25, r_{0,50} = 0.1, r_{0,200} = 0.03, \text{ and } r_{0,900} = 0.005$), also based on fits to the brightest observed clusters. We have also included a cluster model that mimics the typical Galactic globular cluster, with $c = 1.3$ and $r_0 = 1$ pc, equal to 0.1 pixel at the distance of NGC 3597.

To simplify later comparison to the observational data, we have created the artificial clusters for each function with signal-to-noise values which correspond to a range of magnitudes from $R=15$ to $R=25$ in steps of 1 magnitude in our data set of NGC 3597 (total exposure time of ~ 5000 s in each filter); these correspond to S/N ratios of $\sim 5750, 3600, 2300, 1450, 900, 600, 400, 230, 150, 90, \text{ and } 55$ in the F702W filter. We have assumed a color that is the mean of the blue cluster colors from our observations. Since we have based our simulations on the sizes of the brightest clusters in the closer galaxy, NGC 3597, any output radial parameter corresponds to an actual physical size which is $\sim 50\%$ larger in the more distant galaxy, NGC 1275. Since the background is relatively faint for many of the observed clusters, none of these simulations include noise due to the galaxy background, which varies depending on position; for fainter clusters the measured spread should be taken as a lower limit.

Initially, each artificial cluster was fit using the same PSF and model function with which it was constructed, solving for the best fitting radial parameter. Figure 2 shows histograms of the spread in the output radial parameters for the different functions, radial parameters, and magnitudes. From these data we can see that if the cluster light is well modeled by any of the functions we have chosen, the fit given by that function will provide an estimate of the radial parameter of the cluster

which is accurate to better than $\sim 10\%$ for signal-to-noise ratios greater than ~ 100 . There is possibly a small systematic error introduced for the faintest clusters with some of the King models, but it is not particularly large; as we will see later, other uncertainties probably lead to larger systematic errors.

To observe the extent to which it is possible to differentiate between different concentrations we have constructed 11 sets of 100 synthetic clusters with signal-to-noise ratios in the range of 60 - 6000 for the F702W PSF. For each, the input model consists of a King model with $c = 2$ and $r_0 = 0.07$ pixels, as motivated by our fits to the brighter observed clusters in our NGC 3597 data, discussed below. We fit these using King models with different concentrations, and define the output concentration to be the one that gives the best fit; Figure 3 shows histograms of the recovered concentration. While even for the brightest artificial clusters there is difficulty distinguishing between concentrations of 1.7 and 2, only for signal-to-noise ratios below about 150 ($R = 23$) do we find the correct concentration ($c = 2$) in much less than about 50% of the artificial clusters.

Another set of models was constructed with properties based on Galactic globulars as they would be seen at the distance of NGC 3597, to see whether we can derive concentrations for more compact clusters. Eleven sets of artificial clusters were created with the same signal-to-noise range as the previous tests but with different King model parameters ($c = 1.3$, $r_0 = 0.1$ pix, F702W PSF). Histograms of the best fit output concentration are shown in Figure 4. The input concentration is found to be the best fit concentration more than 50% of the time only above a signal-to-noise of ~ 600 , reflecting the fact that constraining the concentration is more difficult for more compact clusters. For the clusters that mimic Galactic globular cluster structural parameters, the tidal radius extends only two pixels from the core for this model, compared to ~ 5 pixels for the artificial clusters based on the parameters of the brightest NGC 3597 clusters.

To determine how much the ability to measure radial parameters is improved if one looks at less distant objects, we also constructed a set of clusters which would represent the expectation for Galactic globulars at the distance of Virgo ($c = 1.3$, $r_0 = 0.28$ pix, F702W PSF). For these input parameters we recover the proper concentration $\sim 50\%$ of the time down to a signal-to-noise of ~ 90 . We show a histogram of the best fit concentrations as a function of signal-to-noise in Figure 5. It is clear that it is far easier to distinguish between different concentrations in instances where the angular size is larger.

We note that in Figures 4 and 5 even at high signal-to-noise some small number of clusters are apparently best fit by $c = 2.3$ or 2.95 . This presumably arises because the algorithm occasionally converges to an incorrect local χ^2 minimum. It only occurs when fitting clusters with small input concentrations. Because it happens only rarely, we have not pursued modifications to the algorithm to avoid the problem.

When we fit lower signal-to-noise artificial King model clusters with King models of different concentrations, we find that the resultant fits are, in a χ^2 sense, equally valid. At lower signal-to-

noise there is a degeneracy among the family of King models which makes uniquely determining a concentration for a given cluster impossible. King models with larger concentrations have smaller output radial parameters. This problem is more notable for more compact clusters. This systematic trend can lead to errors in the output King radii that are correlated with the chosen concentration. To avoid these errors as much as possible, we have followed the example of Kundu & Whitmore (1998), who noted exactly the same effect, and chosen to use the half-light radius, r_h , for cluster-to-cluster comparisons for fainter objects. This quantity is relatively independent of the chosen combination of concentration and King radius.

3.2. Effect of Errors in the PSF

All results above assumed that we have a perfect understanding of the HST/WFPC2 point spread function. To attempt to put some limits on the potential errors arising from an inaccurate PSF model, we have constructed three sets of synthetic King models using three different PSFs:

1. our nominal PSF model (PSF1)
2. a defocussed PSF (PSF2)
3. a PSF from the edge of the PC image (PSF3)

The model clusters for this experiment had $r_0 = 0.07$, $c = 2$, and signal-to-noise ratios ranging from ~ 600 to 55.

We fit each set of artificial clusters using PSF1. The artificial clusters created with PSF2 are reasonably well fit with PSF1 models, with reduced χ^2 values differing significantly from 1 only for $S/N \gtrsim 400$. As might be expected, however, the use of an incorrect PSF can lead to systematic errors. The average output King radii from these fits was 0.082, 17% larger than the input value of 0.07. Fits to clusters made with PSF3 are less accurate, with reduced χ^2 values significantly different from 1 for $S/N \gtrsim 150$. Still, the output best fit radii average is 0.074, only 6% larger than the input King radii. We conclude that while focus and position dependent distortions may contribute to errors in the correspondence between the theoretical profile and the observations, they change the derived radial parameters only slightly.

To determine the potential extent to which our best fitting concentrations may be in error due to variations in the PSF, we constructed sets of artificial clusters using PSF3 and fit them using PSF1. To span the range of parameters that we might encounter when fitting for radial parameters of globulars, we chose two models, one of which represents the parameters expected for young clusters based on our fits ($c = 2$, $r_0 = 0.07$) and the other predicted parameters for an old cluster at the distance of Virgo ($c = 1.3$, $r_0 = 0.28$). We show the histograms of the best fitting output concentrations for the young clusters at the distance of NGC 3597 and the old clusters at

the distance of Virgo in Figures 6 and 7, respectively. From these we can see that for clusters such as those in our observations, an inaccurate PSF can lead to systematic errors in the derived concentration. Using clusters created with PSF3 and fit with PSF1 we find that we would end up selecting a larger concentration for our artificial young clusters at the distance of NGC 3597 (input $c = 2$, output $c = 2.3$). However, for old clusters at Virgo, which are more resolved, we find little difference in the output concentration between clusters created with PSF1 and PSF3 (though the output King radius is about 8% higher than the input). We also note that in Figure 7, as in Figures 4 and 5, a small number of clusters are seemingly best fit by large concentrations; as with the other figures, this is due to errors in the fits for the smaller concentrations.

3.3. Variation with Filter Choice

The F450W filter provides a slightly better discriminant between different concentrations for identical signal-to-noise values because of the better resolution provided at shorter wavelengths. However, in our data sets, for any given magnitude, the F702W filter has significantly higher counts ($\sim 50\%$) than the F450W filter, because of the chosen exposure times and the better quantum efficiency of the PC chip in the red. For the F450W filter to have a higher signal-to-noise for equal exposure times, the cluster would need to have a observed B-R of < -0.5 , which is bluer than even the youngest clusters which have typical B-R colors of -0.4 based on population synthesis models (Charlot & Bruzual 1991). We find for a fixed exposure time, F702W is preferable to F450W for recovering structural parameters. This could probably be generalized to the conclusion that higher signal-to-noise is more important than the slight increase in spatial resolution obtained from observing with HST at shorter wavelengths.

3.4. Discussion

According to our tests, King radii can be measured to an accuracy of 10-15% down to a signal-to-noise of ~ 50 , assuming that sky noise is unimportant and that the concentration is well known. Derivation of the concentration requires substantially higher signal-to-noise because it becomes critical to measure the wings of the objects. Uncertainties in the measured concentration as a function of S/N are shown graphically in Figure 3, Figure 4, and Figure 5. The uncertainty depends on both S/N and the true concentration of the objects; concentration is harder to measure accurately for more compact objects. We find that for young clusters at a distance of NGC 3597 that the input concentration is chosen as the best fit output concentration at least 50% of the time for $S/N \gtrsim 150$. For old clusters at the distance of NGC 3597, the input concentration for the artificial clusters is measured as the best fit output concentration $\sim 50\%$ of the time only for $S/N \gtrsim 900$. For old clusters at Virgo, we find the input concentration as the best fit concentration at the 50% level for $S/N \gtrsim 100$. In each case there is little scatter in the best fit concentration at these S/N ratios (< 0.3 in c or less than a factor of two in the ratio of King to tidal radius), though

the scatter quickly increases at fainter magnitudes. While these are necessarily only errors for discrete combinations of parameters, they do provide some insights into the two most interesting possibilities for the study of globular cluster structural properties, namely, clusters similar to old Galactic globulars and clusters similar to massive young protoglobulars.

While our tests were performed for clusters at the distance of NGC 3597, they can provide limits for clusters at other distances. Globulars in the Virgo cluster, at about 40% of the distance to NGC 3597, would have a signal-to-noise ratio 2.5 times larger than identical clusters in NGC 3597 for similar exposure times, assuming that the dominant source of noise is Poisson noise in the signal. For an exposure time of 1700 seconds in F702W we could expect to accurately measure the concentration of an old globular at the distance of Virgo 50% of the time down to a magnitude of $R = 25$. At greater distances than NGC 3597, the situation becomes worse, as the clusters get both apparently fainter and smaller, and thus we can derive only lower limits to the spread in parameters. For old globulars at the distance of NGC 3597, even a cluster as bright as the brightest globular in a galaxy like M87 would only have an R magnitude of ~ 22 , corresponding to a signal-to-noise ratio of about 230 (for 5000s exposure time). Thus to accurately determine concentrations for even the brightest old globulars, one would either take substantially longer exposures or study closer cluster systems. As noted above, the fits are better for apparently larger clusters. This suggests that dithering, a way of effectively increasing the resolution, would improve the quality of the results.

Unfortunately, errors in our understanding of the PSF can lead to systematic errors in derived radial parameters. Although our simulations suggest that such errors are not extremely large, they are probably responsible for the largest source of uncertainty in our results on observed clusters, discussed next.

4. Data

4.1. Observations

We have applied our technique to Hubble Space Telescope Planetary Camera images of NGC 1275 and NGC 3597. The images of NGC 1275 were taken on 1995 November 16 and consisted of five exposures of 200, 1000, and 3×1300 seconds in the F450W filter and five exposures of 200, 900, 1000, and 2×1300 seconds in the F702W filter. The NGC 3597 images were taken on 1997 May 16 and consisted of four exposures of 4×1300 seconds in the F450W filter and four exposures of 1100 and 3×1300 seconds in the F702W filter. Detailed studies of the blue cluster systems in NGC 1275 and NGC 3597 have been presented in Carlson *et al.* (1998) and Carlson *et al.* (1999), respectively.

For our sample of clusters we have chosen 146 objects from the PC field of NGC 3597 and 255 objects from the PC field of NGC 1275. These subsamples were selected from the list of all clusters in the PC with $B < 26$. All objects with bright neighbors or rapidly varying galaxy

background levels were rejected. This rejection was based on visual inspection of the images and the light profiles of the candidate objects. Objects in the WFs were not included because the poorer resolution of these frames would make fitting for radial parameters more difficult.

4.2. Fitting Radius

The output radial parameters from our fitting program are somewhat sensitive to our choice of fitting radius. We believe that this is a result of inaccuracies in the assumed PSF at small radii. We attempted fits of the clusters using 4 different apertures of 2, 4, 6, and 8 pixels in radius. Figure 8 shows the output King radii for 21 of the brightest clusters as a function of the different fitting radii. The variation of the output radial parameter is less than 50% for all but three of the clusters. The 2 pixel aperture varies to the largest extent, with the greatest deviation between the two and eight pixel aperture being 81%. This supports the hypothesis that the problem arises from PSF inaccuracies at small radii. The biggest deviation between the fit for a four pixel aperture and an eight pixel aperture is only 31%. We adopted 8 pixels as our final fitting radius; note that an 8 pixel radius includes $\sim 94\%$ of the light of an ideal point source (Holtzman *et al.* 1995).

4.3. Accuracy of the Fits

Another test of the accuracy of our models is the uniformity of radial parameters between the two different filters. In Figure 9 we show the output King radius in R plotted against the output King radius in B for a King Model ($c = 2$) fit to the clusters in NGC 3597. Figure 10 shows an identical plot for NGC 1275. The clusters with $B < 23$ are shown as filled circles, while the remaining clusters with $B < 26$ are shown as open triangles. The solid line indicates where the clusters would fall if the King radii were identical in B and R. Note that there is good agreement for the King radii of the F450W and the F702W images, particularly for the higher signal-to-noise clusters. The agreement degrades at fainter magnitudes, but this is probably due to Poisson noise in the signal and sky noise for the fainter objects. One of the brighter clusters in the NGC 1275 images lies well away from the observed correlation. This cluster, with a King radius of 0.19 pixels in the B image and 0.03 pixels in the R image is close (within ~ 12 pixels) to the two brightest clusters in our sample and the best fit King radii may be affected by the wings of those clusters.

If our models for the cluster light distribution and PSF are accurate, we would expect output reduced χ^2 values that are close to one. However, reduced χ^2 values for the brightest clusters which are most sensitive to poor models are dramatically larger than one. In fact, many of these values are larger than we observed even from the simulated PSF errors, as shown in Figure 11. The dominant source of error may well be problems with the PSF model at small radii. Evidence to support this comes from Figure 8 where the fits to the young clusters within two pixels generally deviate more than any other aperture from the general trends. More direct evidence from the

output χ^2 images indicates that the largest part of the error in the fits comes from within a 2 pixel aperture. Unfortunately, since the observed χ^2 are larger than any of those from the simulations, the uncertainties in our results may be larger than we can estimate from the simulations.

4.4. Results - Radii and Concentrations

We present histograms of the derived sizes for 8 different models in Figure 12 for NGC 3597 and Figure 13 for NGC 1275. In each plot the top two boxes show the output half width at half maximum (HWHM) for the Gaussian fits and the output core radii for the modified Hubble profiles. The next six boxes show the output King radii of the clusters assuming they have concentrations of 1, 1.3, 1.7, 2, 2.3, and 2.95, respectively. The final box shows the distribution of King radii for Milky Way globular clusters based on the compilation of Harris (1996). Note that the values of the King radii for the Galactic globular clusters are based on simultaneously fitting for both the King radius and the tidal radius.

Results of trying to derive the concentration are shown in Figure 14, which shows the output reduced χ^2 for the 24 brightest clusters in NGC 3597 as a function of the concentration used in the model. The brighter clusters appear to be best fit with concentration of 2, though it is only slightly preferred over 1.7. Note that the reduced χ^2 values are substantially different from the reduced χ^2 values of the simulations, presumably because the model PSF is not identical to the actual observed PSF as was the case for the simulations. Unfortunately, this allows for the possibility of systematic errors in our derived parameters.

It is clear from these plots is that we can only determine concentrations for the brightest clusters in our sample; this is expected from the simulations given the observed signal-to-noise ratios of the observed clusters. For the vast majority of the clusters in our sample we cannot determine concentration and the King radius simultaneously. Based on the derived concentrations of the brightest few clusters, young blue globular clusters may have concentrations of ~ 2 , corresponding to a ratio of tidal to King radius of 100. The typical Galactic globular cluster has a concentration of about 1.3 (or a ratio of 20). Based on these few clusters, it is difficult to definitively say if young globulars are truly less centrally concentrated than old globulars.

Since we can only uniquely determine the concentration for a few of the brightest clusters and the derived value for the King radius is correlated with the concentration used for the fit, we cannot uniquely determine King radii for fainter objects. To provide a model-independent size estimate, we have adopted the solution of Kundu & Whitmore (1998) and measured the half-light radius, r_h , for the clusters, which is only weakly dependent on adopted concentration. We have determined the half-light radius as a function of King radius using the $c = 2$ King model fit by numerical integration of the model. Using this result, we convert the best fit King radius into a half-light radius. The use of the half-light radius simplifies comparison to Galactic globular clusters, and we present histograms of half-light radii for NGC 3597, NGC 1275, and the Galactic globular cluster

system in Figure 15. We find the massive young clusters in both NGC 3597 and NGC 1275 have half-light radii that clearly place them in the same size range as Galactic globular clusters. The mean sizes may be slightly larger than those of Galactic globulars; similar results were obtained for the young clusters in NGC 4038/4039 (Whitmore *et al.* 1999).

4.5. Correlations of Sizes with Other Cluster Properties

In Figure 16 we display the R magnitude as a function of half-light radius for the young clusters in NGC 3597 and NGC 1275. Since most of the clusters in each galaxy have similar colors (hence similar stellar populations), the R magnitude is probably a rough mass indicator. Error bars for the cluster sizes are plotted using error estimates from our simulations based on the S/N; as noted above, systematic errors may also exist that we cannot estimate. While no obvious trend emerges, we do find that the plots look similar to a plot of M_V versus half-light radius for the globular clusters in the Milky Way. Clusters with smaller half-light radii span the whole range of magnitudes, while larger clusters are preferentially fainter. Similar results were obtained for old globular cluster systems around NGC 3115 (Kundu & Whitmore 1998) and M87 (Kundu *et al.* 1999).

To investigate the possibility that the size of the young clusters may be correlated with position in the galaxy, we have plotted the distance from the galaxy centers against the half-light radii of the clusters in NGC 3597, NGC 1275, and the Milky Way in Figure 17. Note that clusters in the Galactic sample are plotted to much larger distances than for NGC 3597 and NGC 1275; the distance to which we can measure accurate sizes is limited to the size of the PC chip in the WFPC2 observations. The corresponding limiting distances to which we have observations are shown in the lower panel as dotted lines; we observe only to ~ 4.5 kpc in NGC 3597 and ~ 8 kpc in NGC 1275. The twenty brightest clusters in each sample are shown as filled circles. Though there is no correlation between galactocentric distance and half-light radius, it is notable that there are no Galactic globulars with half-light radii larger than about 8 pc within 8 kpc from the Galactic center, though some such clusters exist at greater distances from the Galactic center. However, these clusters seem not uncommon in the young cluster samples. Several possibilities exist to explain this discrepancy. Since we only know the projected distance from the galaxy centers in our young cluster sample, some of the clusters may actually be at > 8 kpc. Also, of the twenty brightest clusters with the best determined half-light radii in each galaxy, only 2 have half-light radii greater than 10 pc; some of the clusters may have larger half-light due to inaccurate fits due to low signal-to-noise. The possibility also exists that the clusters within 8 kpc with large half-light radii will be more prone to disruption by effects such as tidal shocks, and as a result, we only expect to see them in younger systems.

4.6. Comparison with Previous Work

Many previous methods of determining the sizes of young clusters have relied on measuring aperture magnitude differences. These magnitude differences are compared to those for models with similar pixel centerings to determine a radial parameter. In this paper, we have directly fit the surface brightness distributions of the clusters with the convolution of a PSF and a variety of different broadening functions. To attempt to better constrain the accuracy of the various different methods of measuring sizes using aperture magnitude differences, we compare the results of a few of the aperture magnitude tests from the literature with our results from direct fits to the data.

Several authors have used direct aperture magnitude differences to determine the structural parameters of young globulars (Whitmore *et al.* 1993, Whitmore & Schweizer 1995, Schweizer *et al.* 1996). The measured aperture magnitude differences between a 0.5 or 0.8 pixel radius aperture and a 3 pixel aperture are compared to the same difference for models of Gaussians convolved with stellar images, which reflect the PSF. In Figure 18 we show $m_{0.8}-m_3$ for the 100 brightest clusters plotted against the output r_0 for the King model fit with $c = 2$ from our fitting program. The general trend confirms that these models can be used to approximate the structural parameters of young globulars, but the scatter suggests that there are potentially large uncertainties judging from the difference in the results from the different techniques.

A potentially more sophisticated technique originally employed by Holtzman *et al.* (1996) uses the aperture magnitude difference between a one and two pixel aperture magnitude for each cluster. A model PSF is constructed with identical pixel centering at the same position in the image, taking into account varying distortions with position. The $m_1 - m_2$ for the model is then subtracted from the observed $m_1 - m_2$. The result is then compared to the same values for modified Hubble profiles of varying core radii convolved with model PSFs. Using this technique it was noted that there is some spread in aperture magnitude differences due primarily to a cluster’s centering within a pixel. In Figure 19 we plot r_0 for King model fits with $c = 2$ against the difference in the aperture magnitude difference between the observed clusters and the PSF. As with the previous method, there is clearly a general trend, but there is also a large scatter. In fact, from this comparison, the differential technique does not appear to do as well as the simpler aperture difference. It is possible, however, that some of the scatter actually arises from the neglect of position dependent PSFs in the *current* fitting method.

5. Summary

We have modeled the surface brightness distributions of 146 young globulars in NGC 3597 and 255 young globulars in NGC 1275 to determine their structural parameters. We have used Gaussians, modified Hubble profiles, and King models as the functional forms for the surface brightness distributions of the underlying clusters and convolved these with optical models of the Planetary Camera PSF.

From simulations, we find that we can reliably retrieve concentrations for $S/N \gtrsim 600$, relatively independently of input radii/concentrations. If the concentration is known or can be derived, we find that the measured King radius is accurate to better than 20% regardless of the values of the parameters down to $S/N \sim 50$. If we use the wrong concentration for a given artificial cluster, the output King radius is systematically wrong. However, if we choose a concentration, the output King radii from cluster to cluster give a reasonable approximation of the relative differences in size. The half-light radius is relatively independent of chosen concentration, and is therefore a less model-dependent estimate of cluster sizes.

We find that there is good correspondence between the measured radial parameters in the F450W and the F702W filters, which suggests that errors in our PSF models are not color dependent. However, the absolute errors represented by the output reduced χ^2 values of the fits to the data are larger than might be expected from simple errors in focus or neglecting the position dependent distortions of the PC field of view. This suggests that our understanding of the PSF could use some improvement. PSF inaccuracies probably are responsible for the largest source of uncertainty in the current results; unfortunately, such errors could be systematic.

We find preliminary evidence that the young clusters in NGC 3597 are less centrally concentrated than the old globular clusters in the Galaxy. This may not be overly surprising, as many forces act to reduce the tidal radii of globular clusters over their lifetimes, particularly evaporation.

Comparing the young clusters to old Galactic globulars, we find that the half-light radius distributions are similar, although the mean size of the young clusters may be slightly larger; the clusters have sizes consistent with their being younger versions of Galactic globular clusters. The distribution of half-light radii in the young cluster systems extends to somewhat larger radii than that of the Galaxy. This may be an evolutionary effect, as larger clusters may be more prone to disruption. We also find some relatively large clusters with relatively small projected galactocentric distance that do not appear to have a Milky Way counterpart. There is no strong correlation between magnitude or galactocentric distance and half-light radius, although there do not appear to be any very bright clusters that are also large.

Significant future progress will require observations of substantially higher S/N to allow measurements of concentrations for a larger number of objects. Spatially dithering of such observations may increase the accuracy of derived radial parameters. Finally, additional work on improving the PSF models may be necessary to increase our confidence on derived cluster parameters.

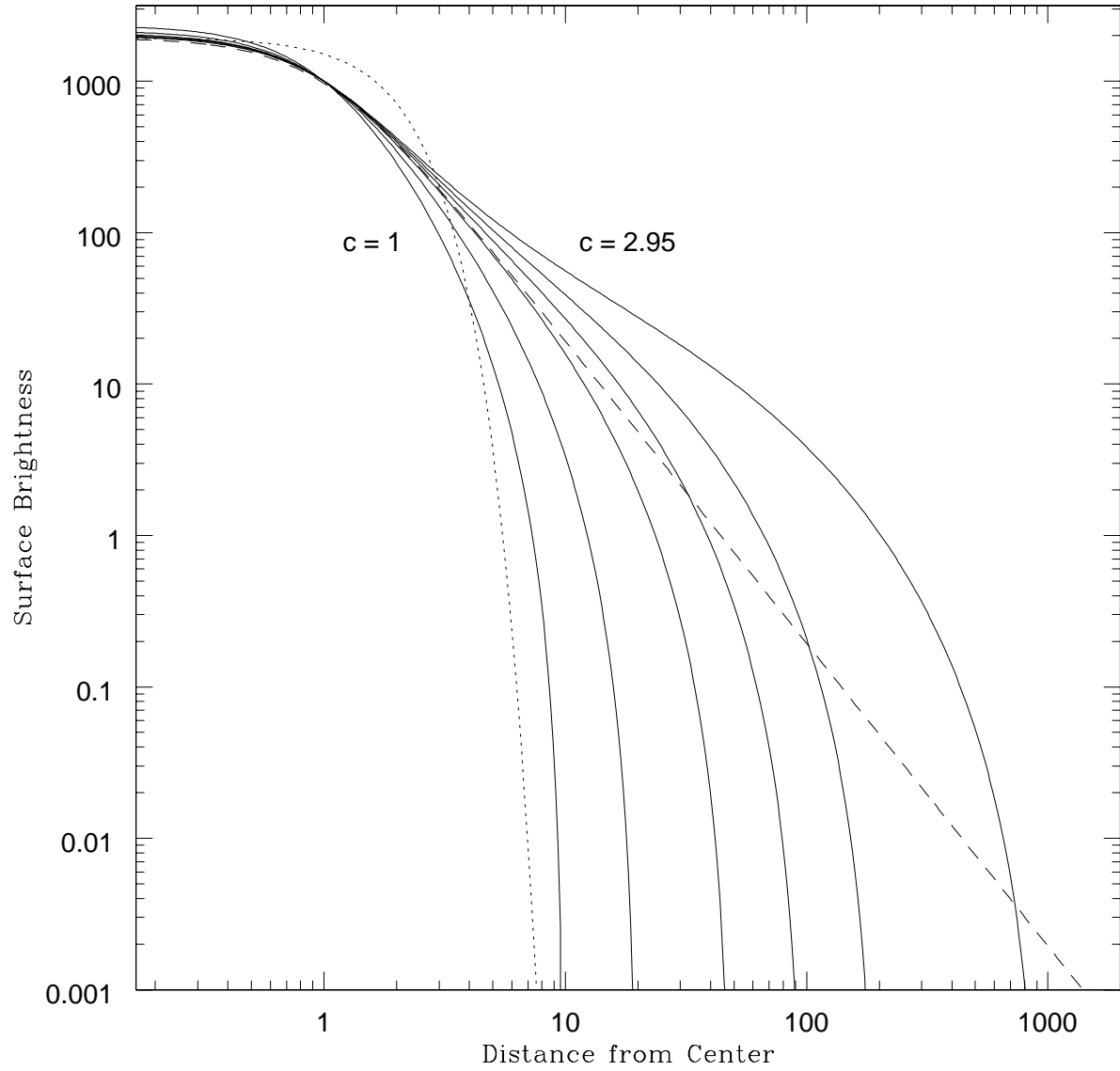
This work was supported in part by NASA under contract NAS7-918 to JPL and a grant to M. C. from the New Mexico Space Grant Consortium.

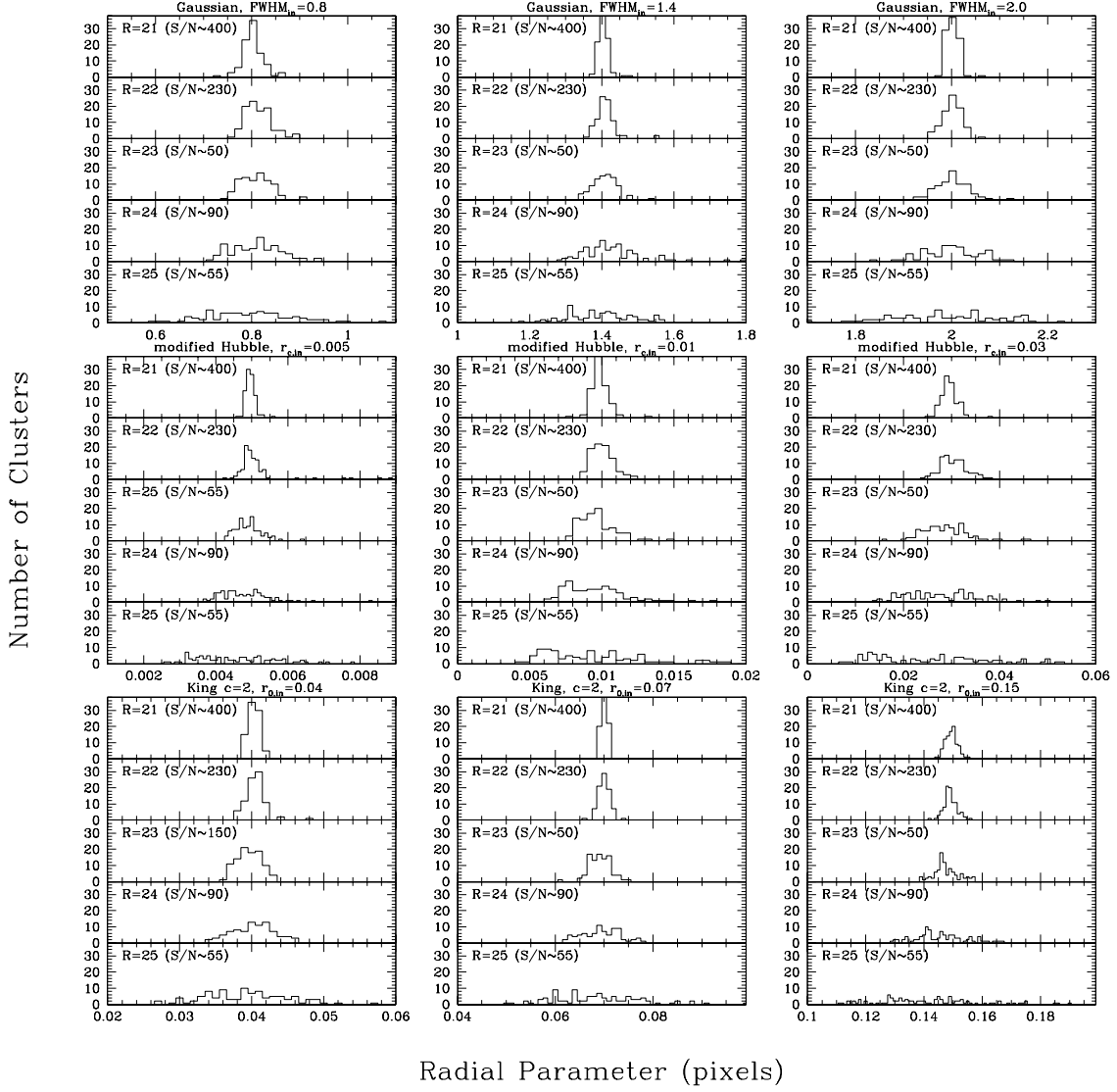
REFERENCES

- Ashman, K. M, & Zepf, S. E., 1998, *Globular Cluster Systems* (Cambridge: Cambridge University Press)
- Burrows, C. J. *et al.* 1995, *Wide Field and Planetary Camera 2 Instrument Handbook*, ed. Burows, C. J. (STScI publication), p. 57
- Charlot, S. & Bruzual, A. G. 1991, *ApJ*, 367, 126
- Carlson, M. N. *et al.* 1998, *AJ*, 115, 1778
- Carlson, M. N. *et al.* 1999, *AJ*, 117, 1700
- Chun, M. S. 1978, *AJ*, 83, 1062
- Crampton, D., Cowley, A. P., Schade, D., & Chayer, P. 1985, *ApJ*, 288, 494
- Demers, S., Kunkel, W. E. & Grondin, L. 1990, *PASP*, 102, 632
- Elson, R. A. W. & Freeman, K. C. 1985, *ApJ*, 288, 521
- Elson, R. A. W. & Schade, D. 1994, *ApJ*, 437, 625
- Harris, W. E. 1996, *AJ*, 112, 1487
- Holtzman, J. A. *et al.* 1992, *AJ*, 103, 691
- Holtzman, J. A. *et al.* 1995, *PASP*, 107, 156
- Holtzman, J. A. *et al.* 1996, *AJ*, 112, 416
- King, I. R. 1962, *AJ*, 67, 471
- King, I. R., Hedemann, E., Hodge, S. M., & White, R. E. 1968, *AJ*, 73, 456
- Kontizas, M. 1984, *A&A*, 131, 58
- Kundu, A. & Whitmore, B. C. 1998, *AJ*, 116, 2841
- Kundu, A., Whitmore, B. C., Sparks, W. B., Macchetto, F. D., Zepf, S. E., & Ashman, K. M. 1999, *ApJ*, 513, 733
- Marquardt, D. W. 1963, *Journal of the Society for Industrial and Applied Mathematics*, 11, 431
- Schweizer, F., Miller, B. W., Whitmore, B. C., & Fall, S. M. 1996, *AJ*, 112, 1839
- Surdin, V. G. 1993, in *The Globular Cluster Galaxy Connection*, ASP Conf. Series Vol. 48, ed. G. H. Smith and J. P. Brodie (San Francisco: BookCrafters, Inc.), p. 342
- Weinberg, M. D. 1993, in *The Globular Cluster Galaxy Connection*, ASP Conf. Series Vol. 48, ed. G. H. Smith and J. P. Brodie (San Francisco: BookCrafters, Inc.), p. 689
- Whitmore, B. C., Schweizer, F., Leitherer, C., Borne, K. & Robert, C. 1993, *AJ*, 106, 1354
- Whitmore, B. C. & Schweizer, F. 1995, *AJ*, 109, 960
- Whitmore, B. C., Zhang, Q., Leitherer, C., Fall, S. M., Schweizer, F., & Miller, B. W., 1999, *AJ*, 188, 1551

Zepf, S. E., Ashman, K. M, English, J., Freeman, K. C., & Sharples, R. M, 1999, AJ, 188, 752

Fig. 1.— Radial plots of six King models (solid lines, King radii of 0.01 and concentrations of 1, 1.3, 1.7, 2, 2.3, and 2.95), a modified Hubble profile (dashed line, core radius of 0.01), and a Gaussian (dotted line, FWHM of 0.01).





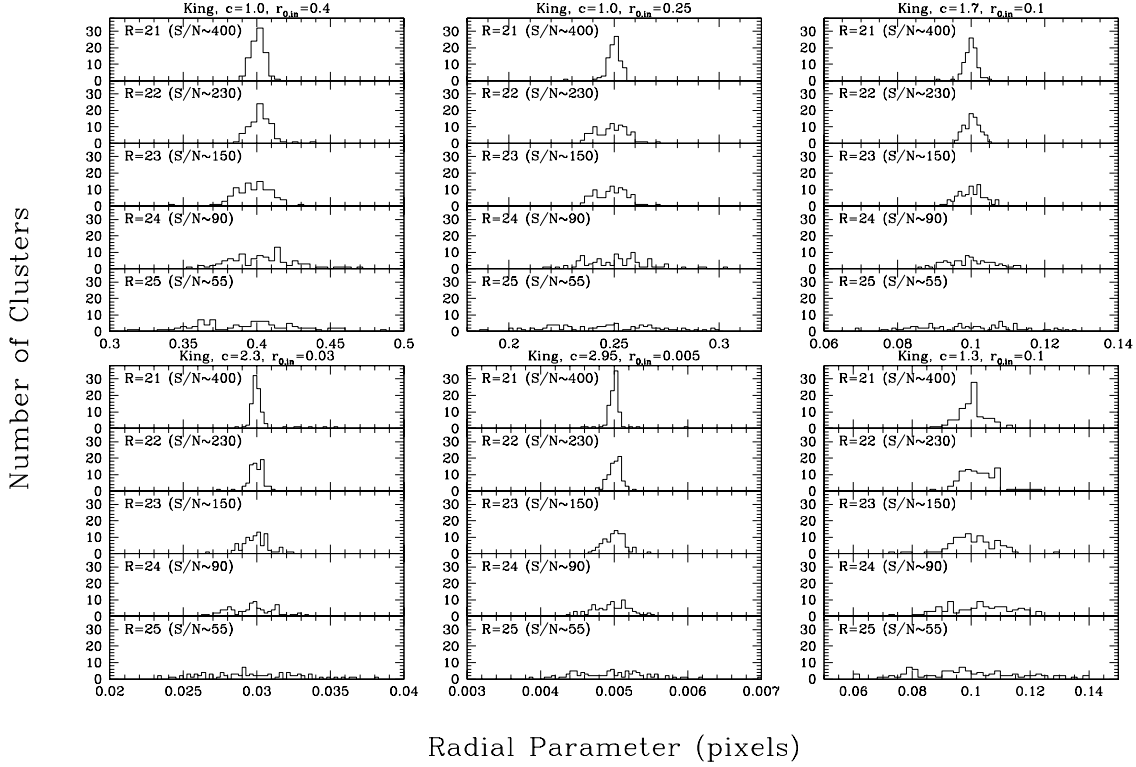


Fig. 2.— Histograms of output radial parameters from fits to synthetic clusters. The radial parameter is the FWHM for the Gaussian, the core radius for the modified Hubble profile, and the King radius for the King models; all radial units are in pixels. Input functions and concentrations for the King models were identical for artificial image construction and fitting.

Fig. 3.— Histograms of best fit concentration as a function of magnitude. Input artificial cluster was given $c = 2$ and $r_0 = 0.07$ pix, typical of blue clusters in NGC 3597.

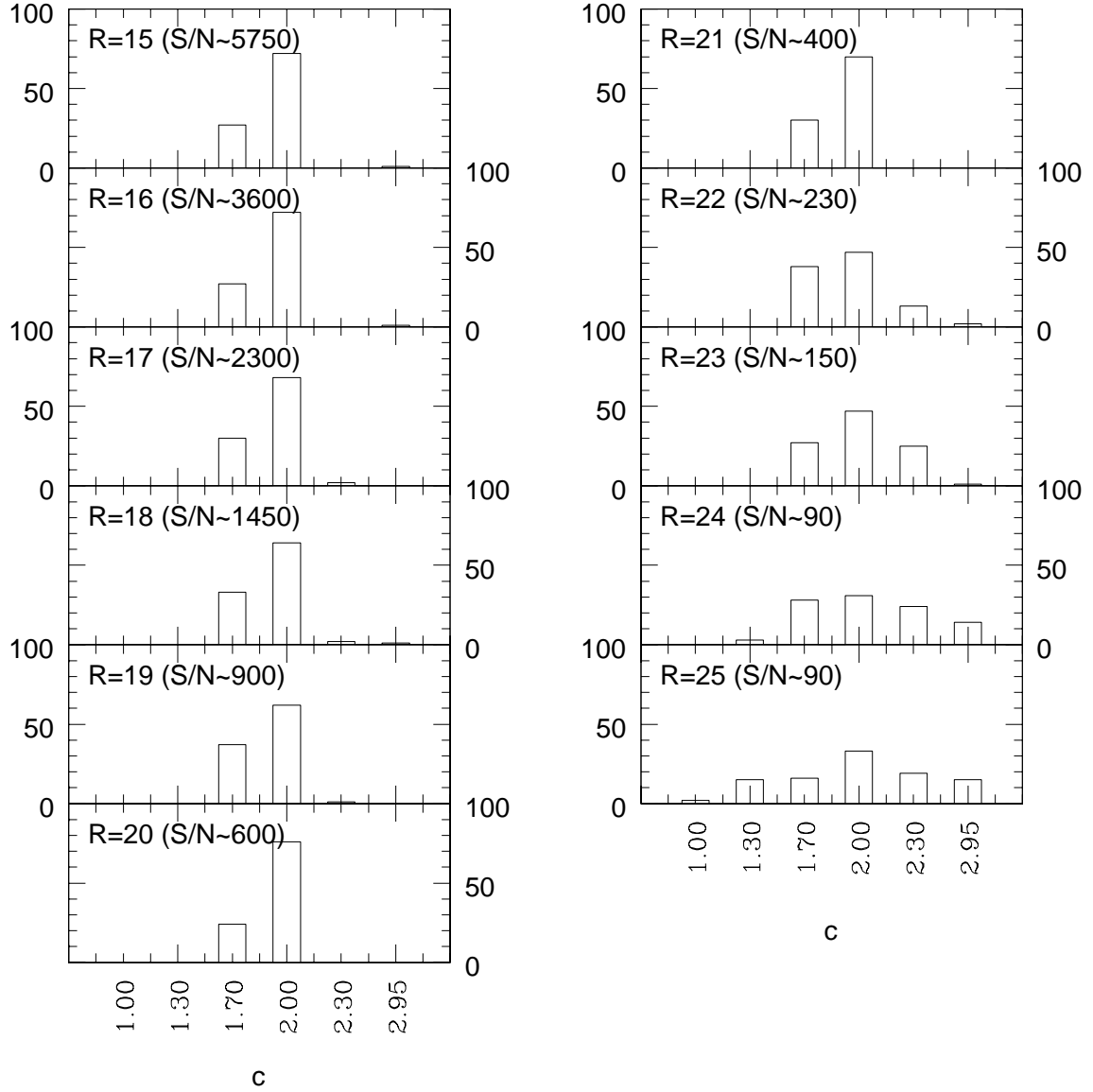


Fig. 4.— Histograms of best fit concentration as a function of magnitude. Input artificial cluster was given $c = 1.3$ and $r_0 = 0.1$ pix, similar to Galactic globular clusters if observed at the distance of NGC 3597.

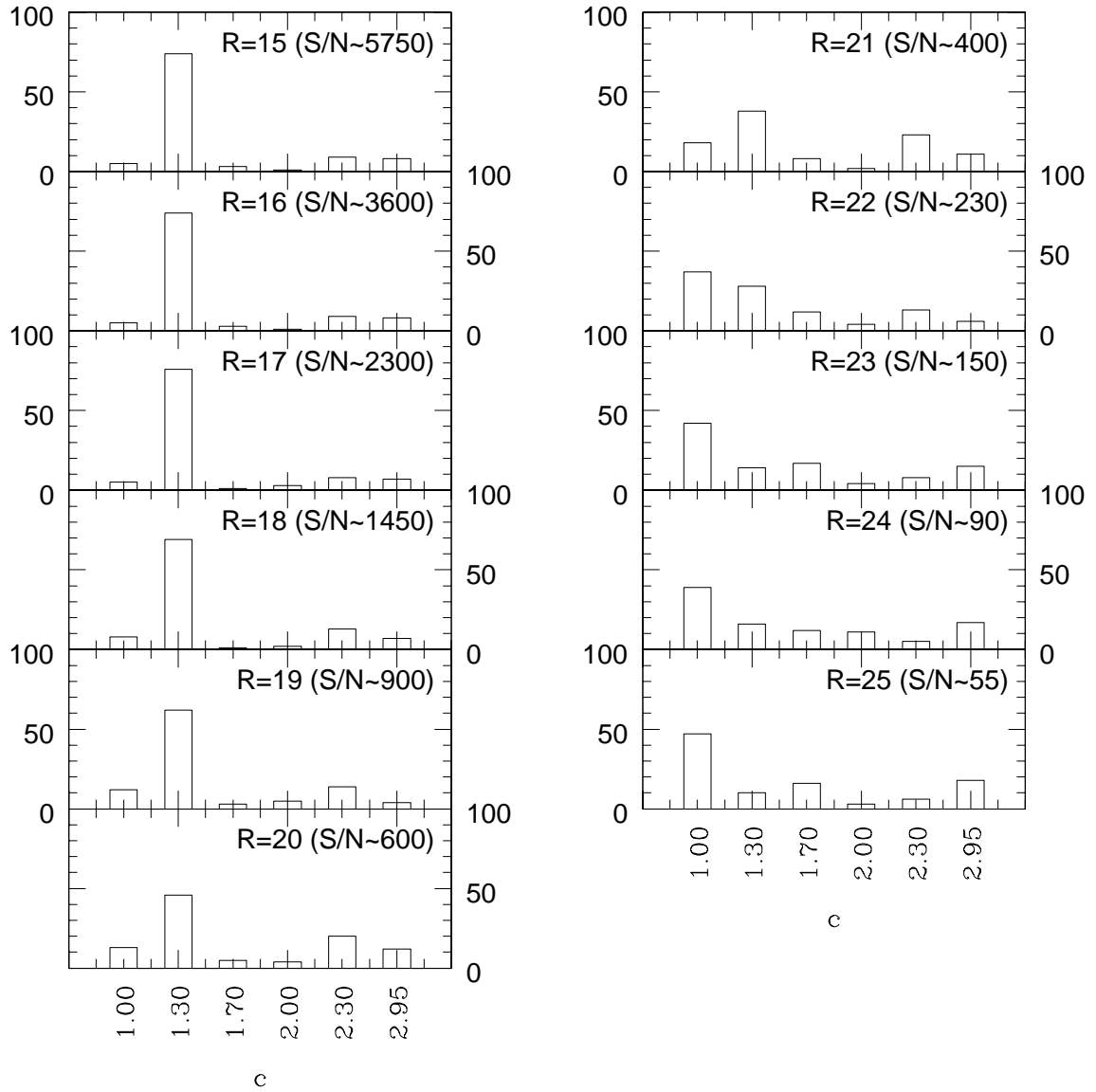


Fig. 5.— Histograms of best fit concentration as a function of magnitude. Input artificial cluster was given $c = 1.3$ and $r_0 = 0.28$ pix, parameters which would be similar to those expected for a Galactic globular cluster at the distance of the Virgo cluster.

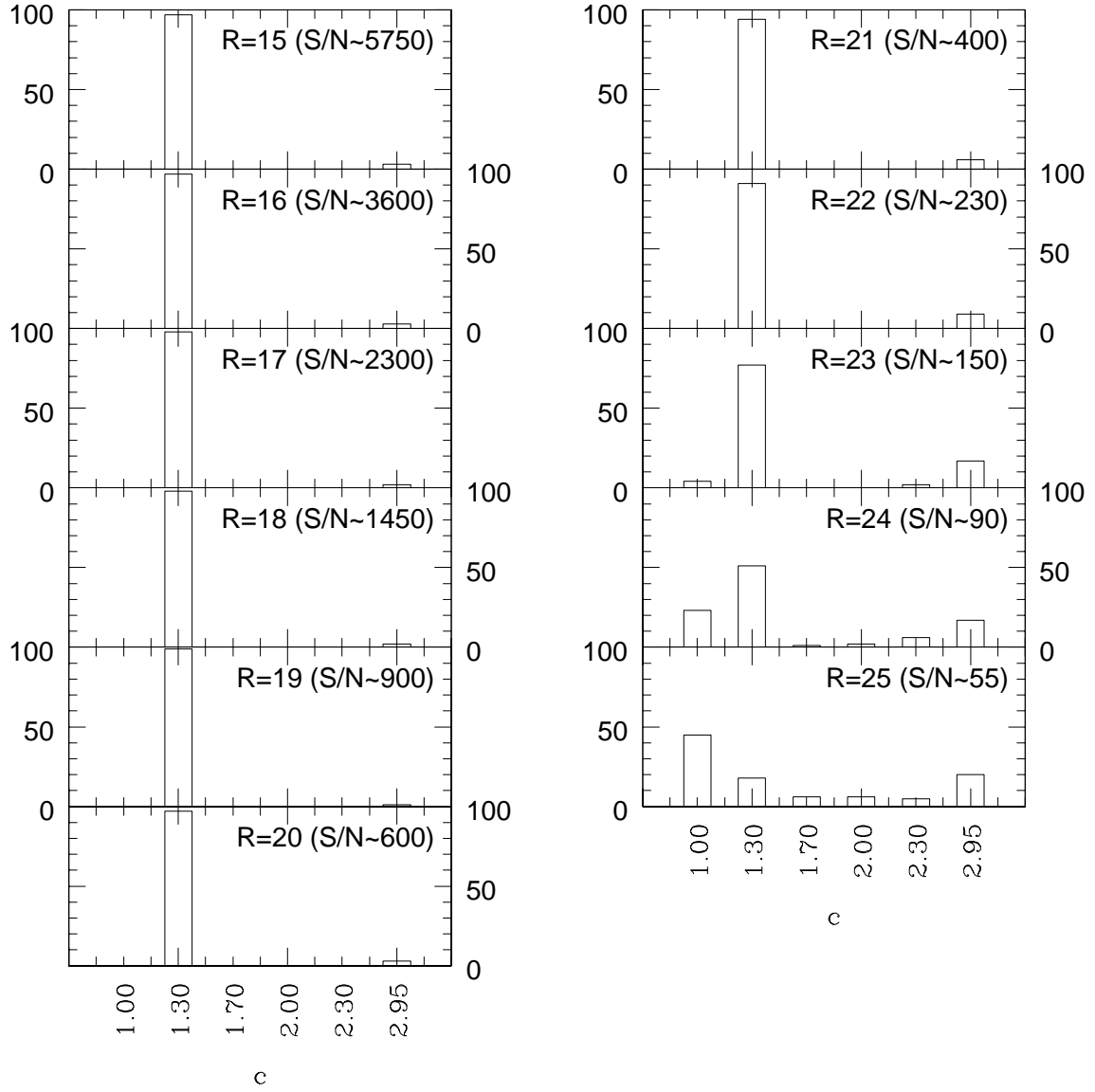


Fig. 6.— Histograms of best fit concentration as a function of magnitude. Input artificial cluster was given $c = 2$ and $r_0 = 0.07$ pix as in Figure 4, but were created using PSF3 and fit using PSF1.

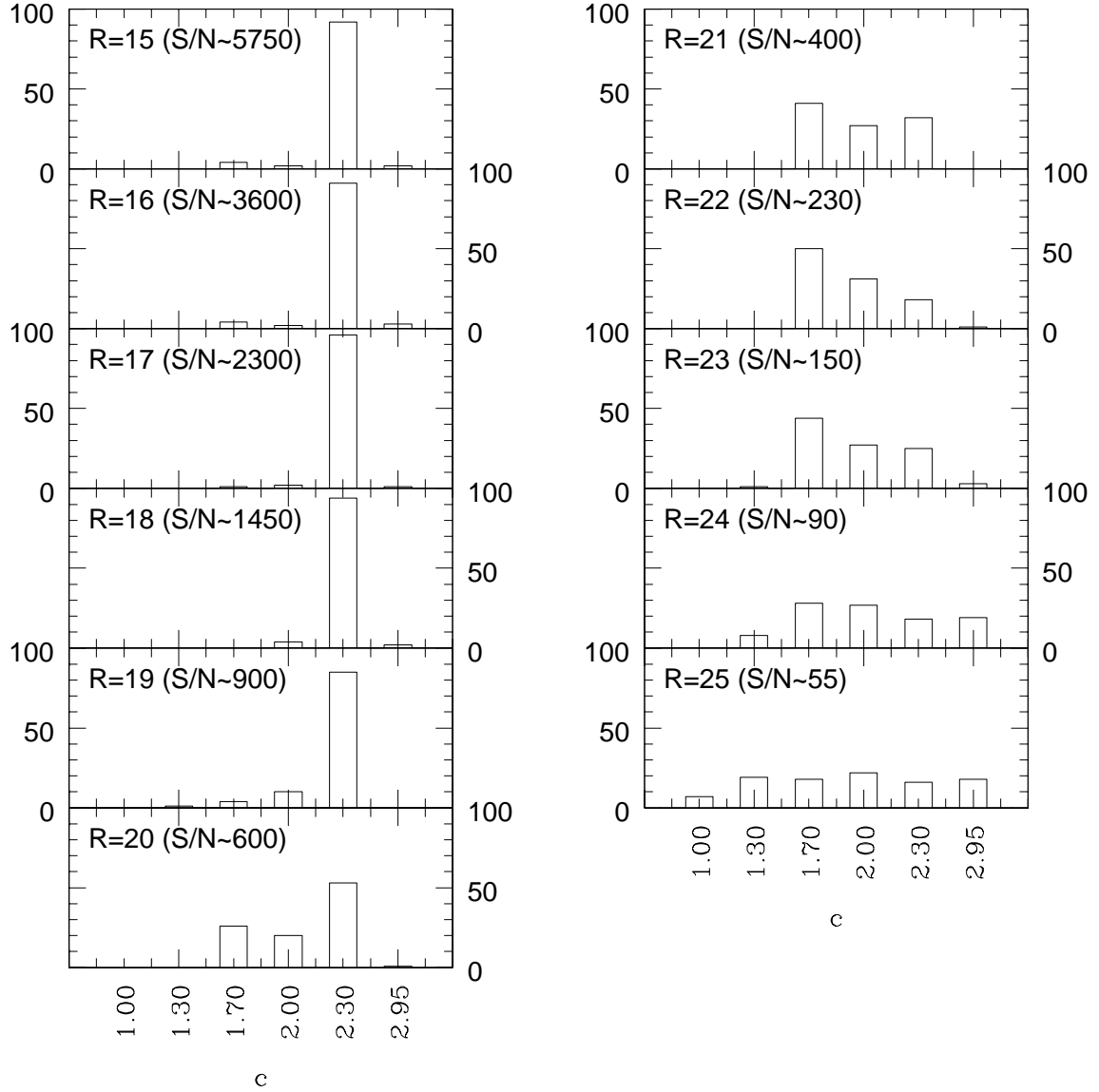


Fig. 7.— Histograms of best fit concentration as a function of magnitude. Input artificial cluster was given $c = 1.3$ and $r_0 = 0.28$ pix as in Figure 6, but were created using PSF3 and fit using PSF1.

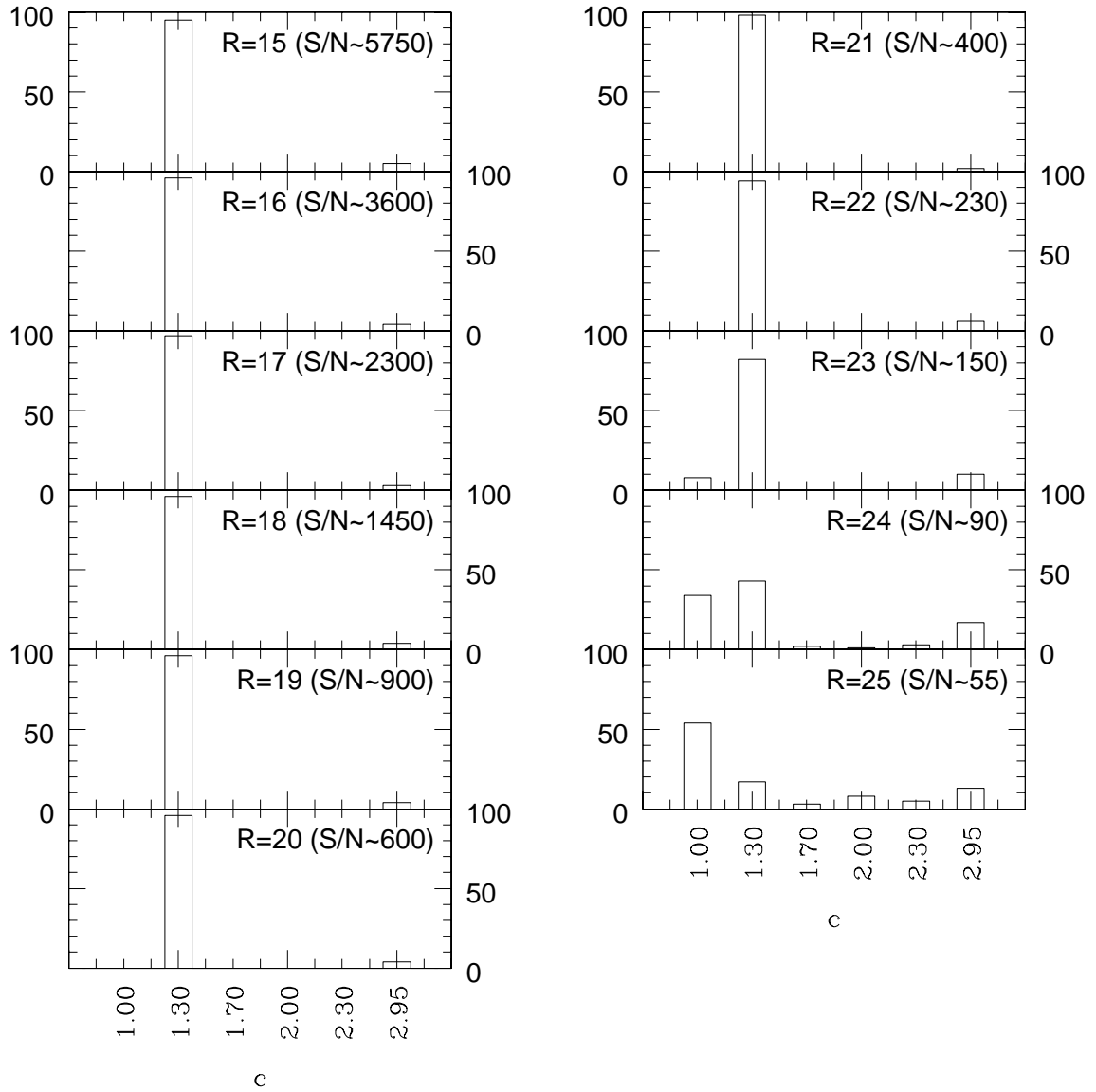


Fig. 8.— Best fit King radius for a $c = 2$ King model vs Fitting Radius for 21 of the brightest clusters. The object with $R = 19.13$ is likely a foreground star.

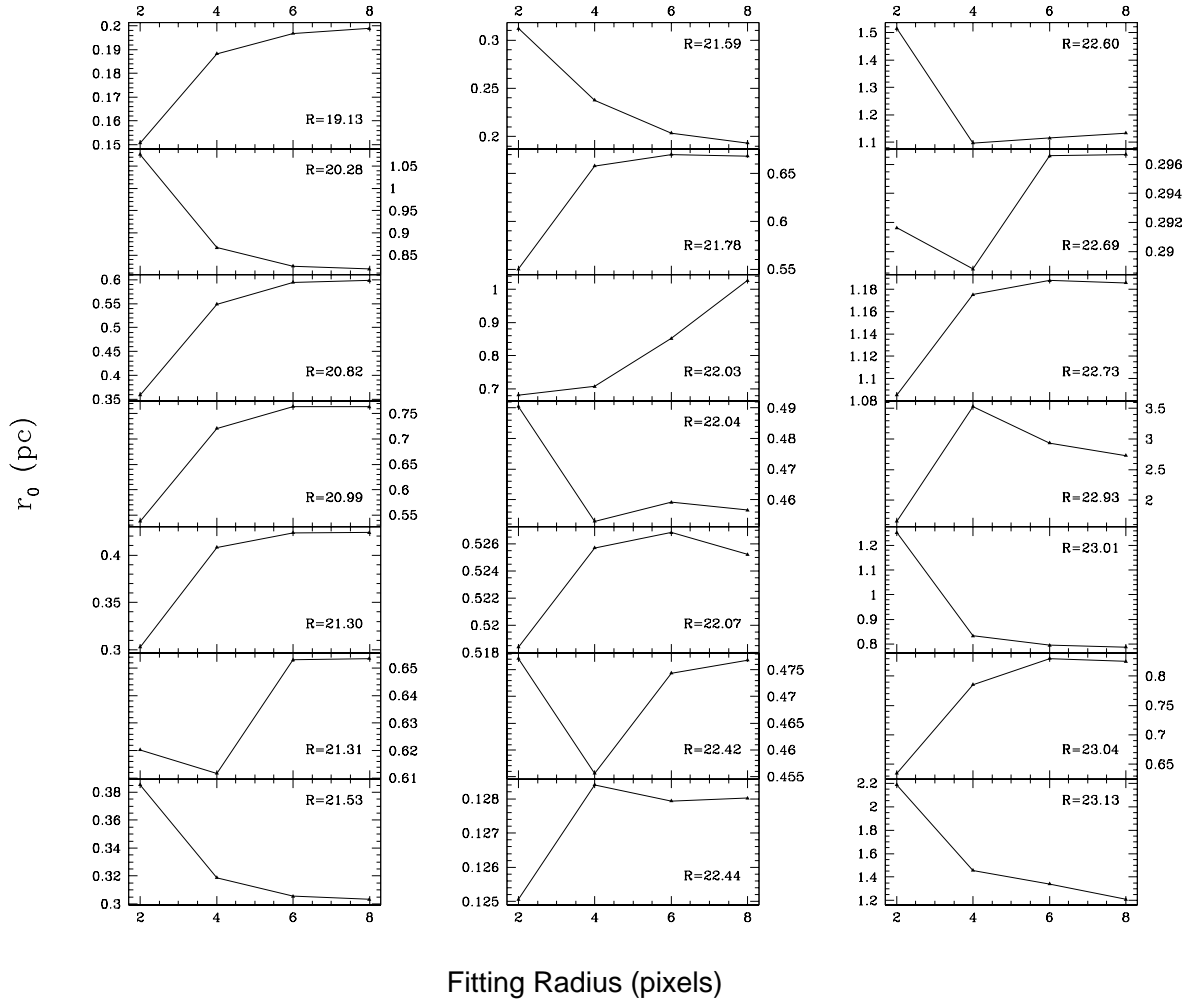


Fig. 9.— Correspondence of King radius in B and R images for NGC 3597. All clusters brighter than $R = 23$ shown as filled circles. Fit was done with $c = 2$ King model.

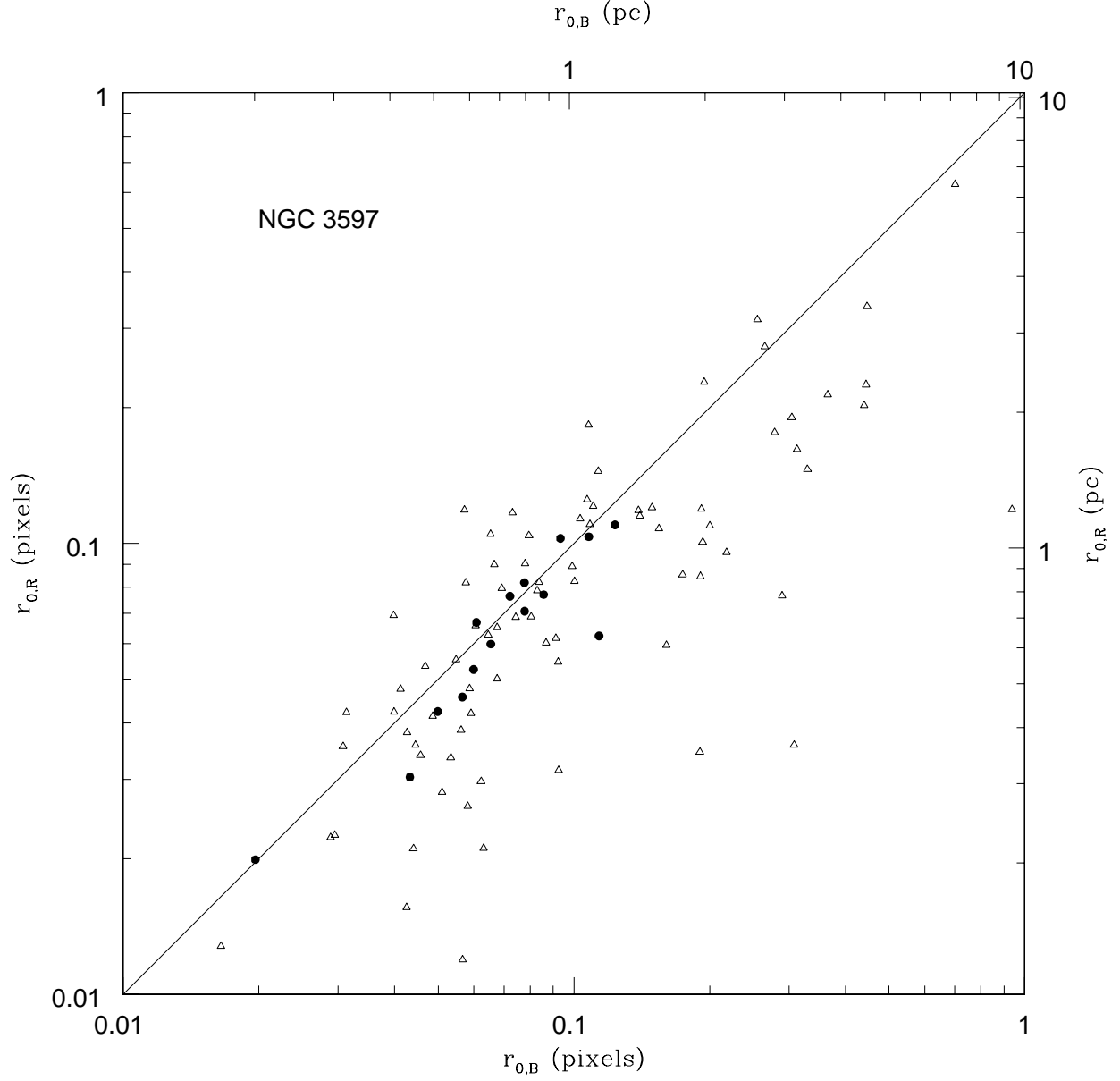


Fig. 10.— Correspondence of King radius in B and R images for NGC 1275. All clusters brighter than $R = 23$ shown as filled circles. Fit was done with $c = 2$ King model.

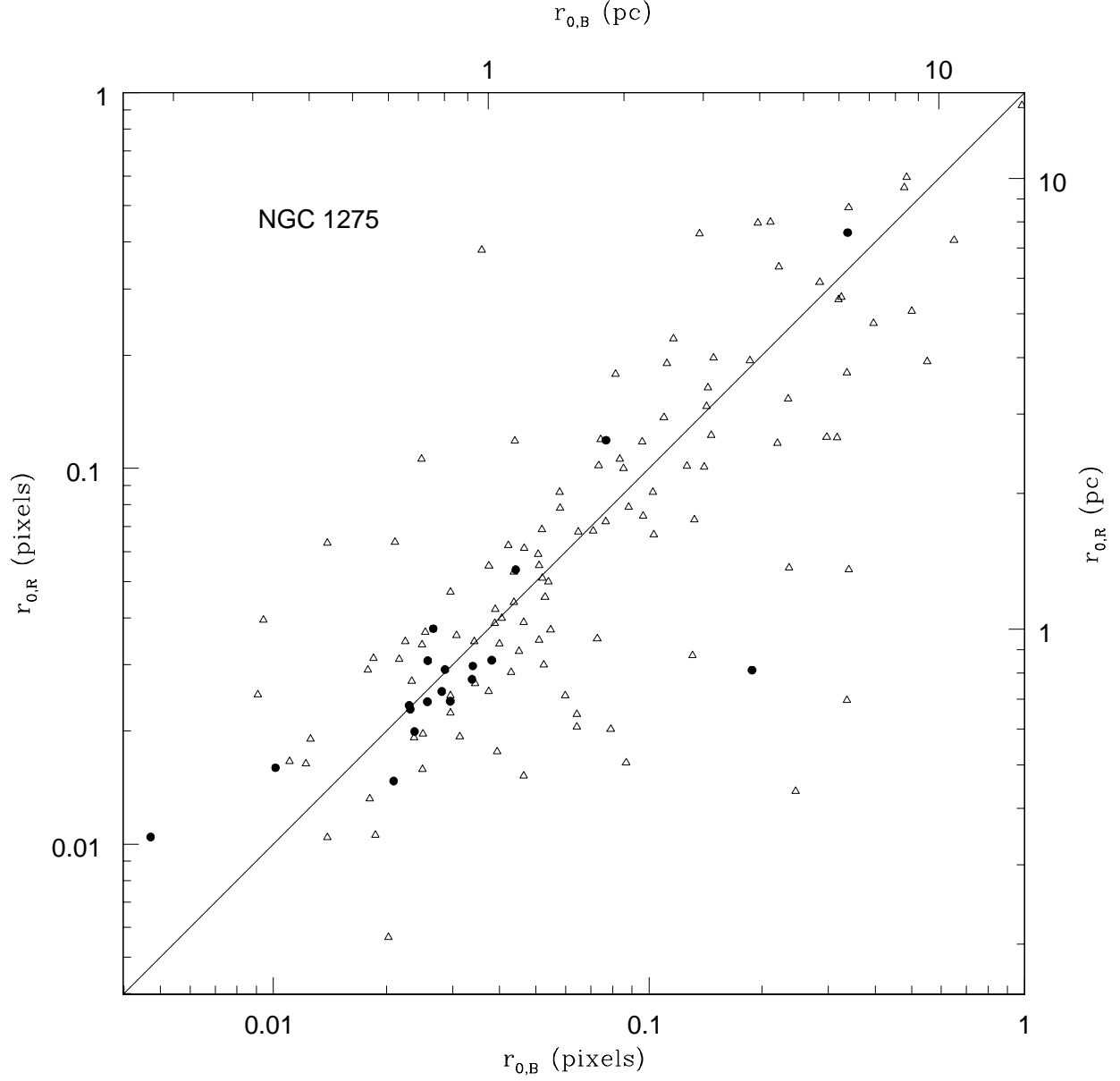


Fig. 11.— Reduced χ^2 for three King models ($c = 2$) vs R magnitude. Output χ^2 connected by lines are from fits to simulations constructed with the specified PSF and fit with PSF1. PSF1 is a sharp focus PSF at the center of the PC image. PSF2 is a poorly focused PSF. PSF3 is a sharp focus PSF at the edge of the PC field. Values for observed clusters in NGC 3597 are shown as filled circles.

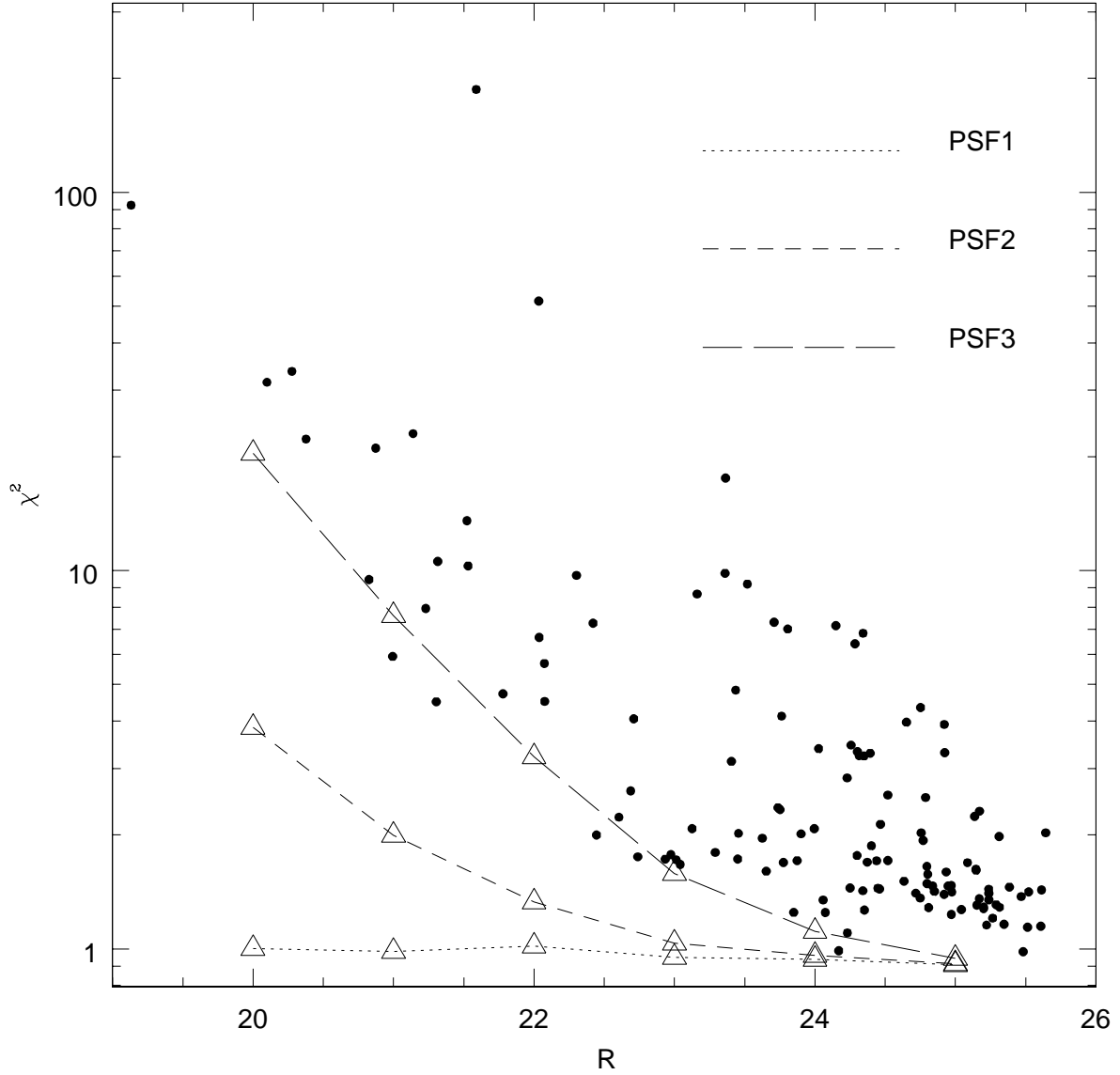


Fig. 12.— Radial parameters of best fits to the clusters in NGC 3597. Milky Way King radii shown for comparison.

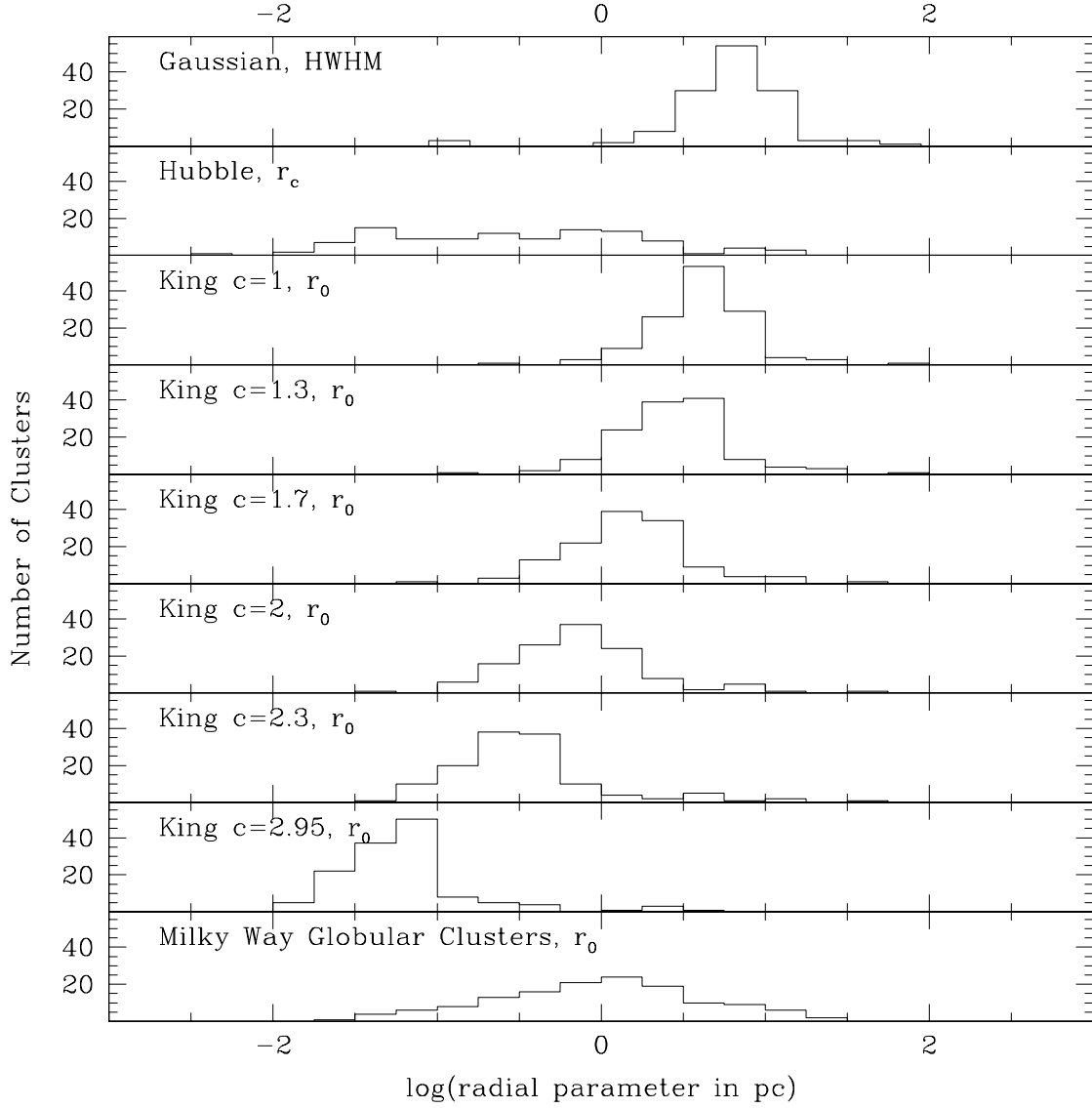


Fig. 13.— Radial parameters of best fits to the clusters in NGC 1275. Milky Way King radii shown for comparison.

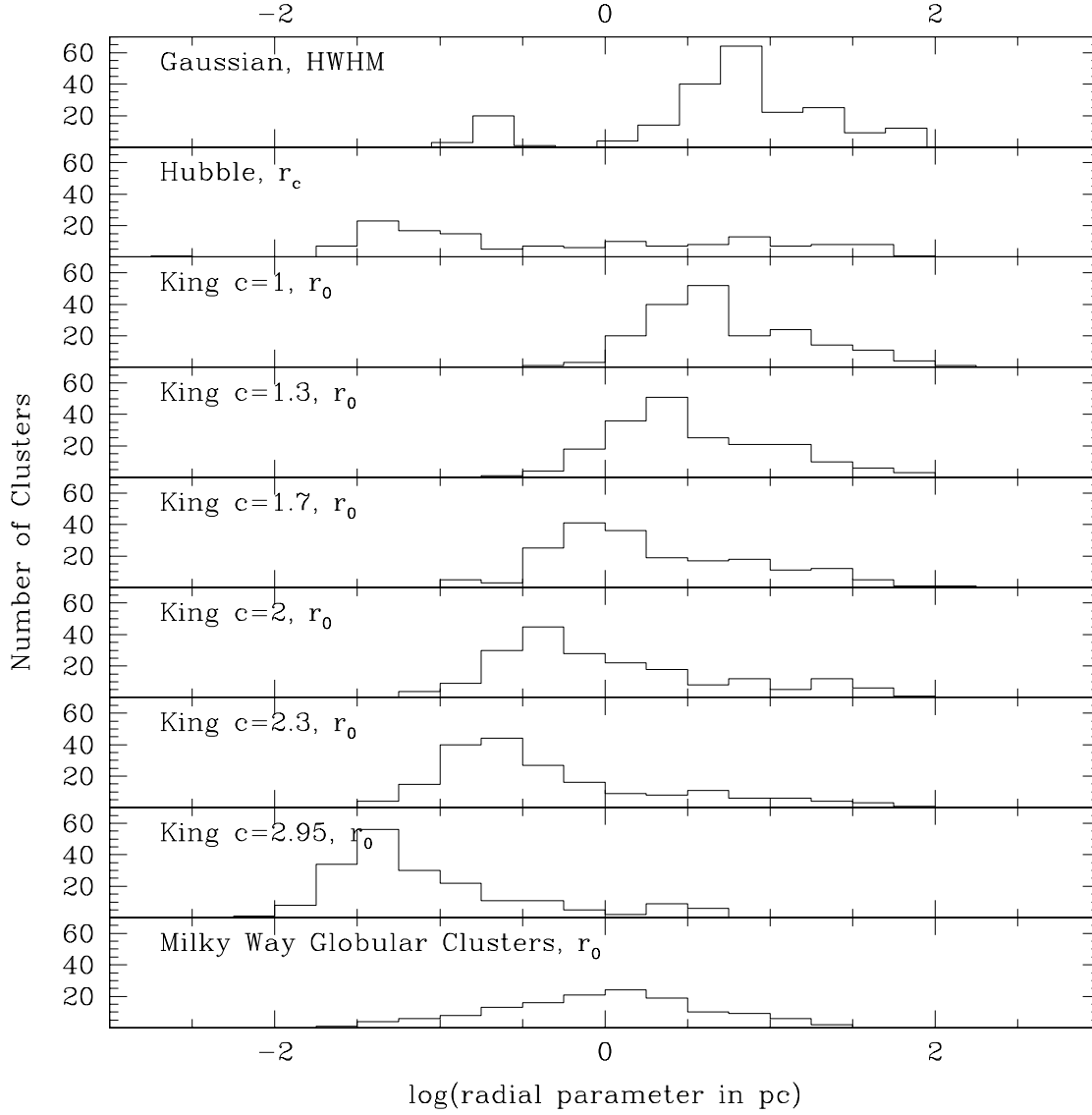


Fig. 14.— Output reduced χ^2 vs concentration for 24 of the brightest clusters. The object with $R = 19.13$ is likely a foreground star.

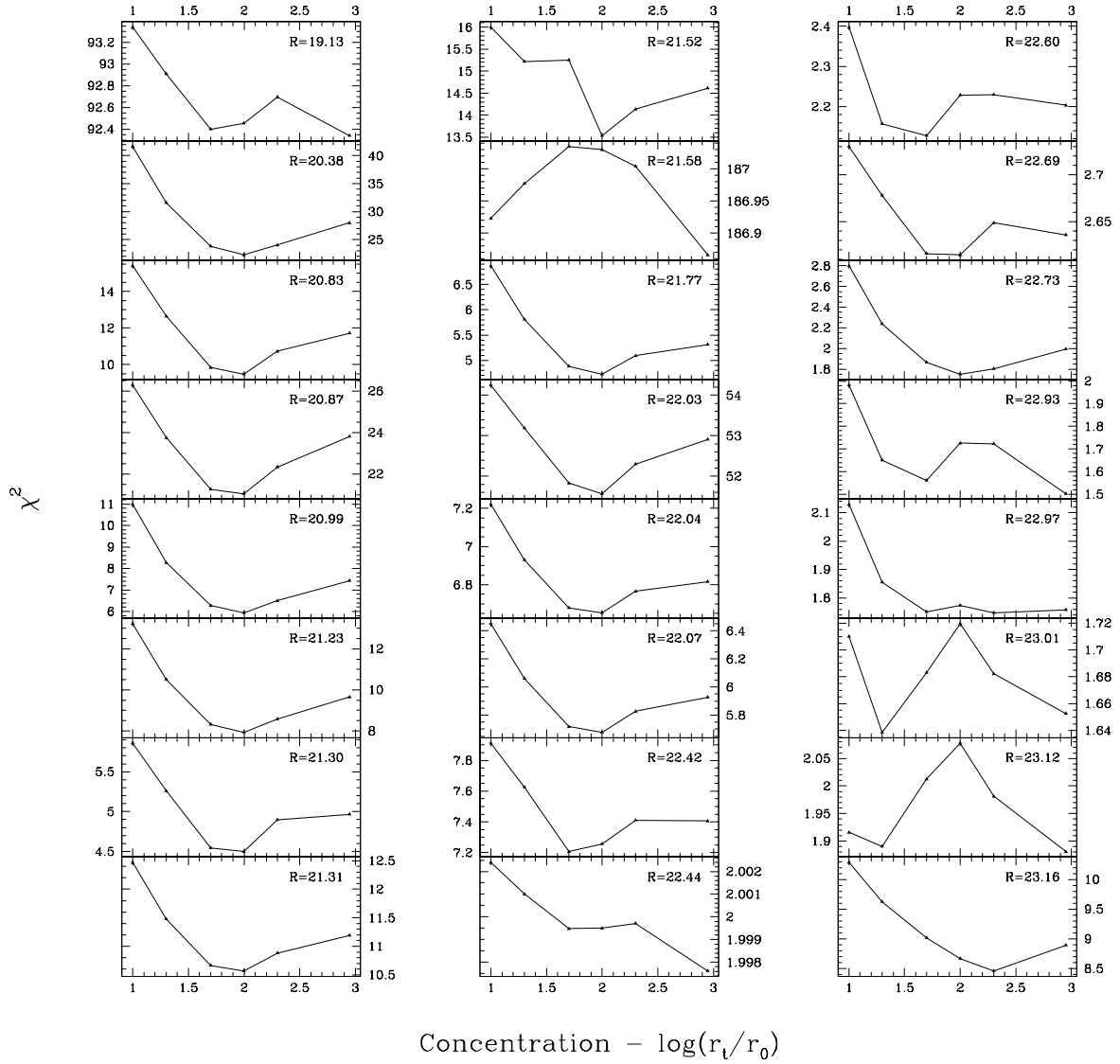


Fig. 15.— Histograms of $\log(\text{Half-light radius in pc})$ for NGC 3597, NGC 1275, and the Milky Way.

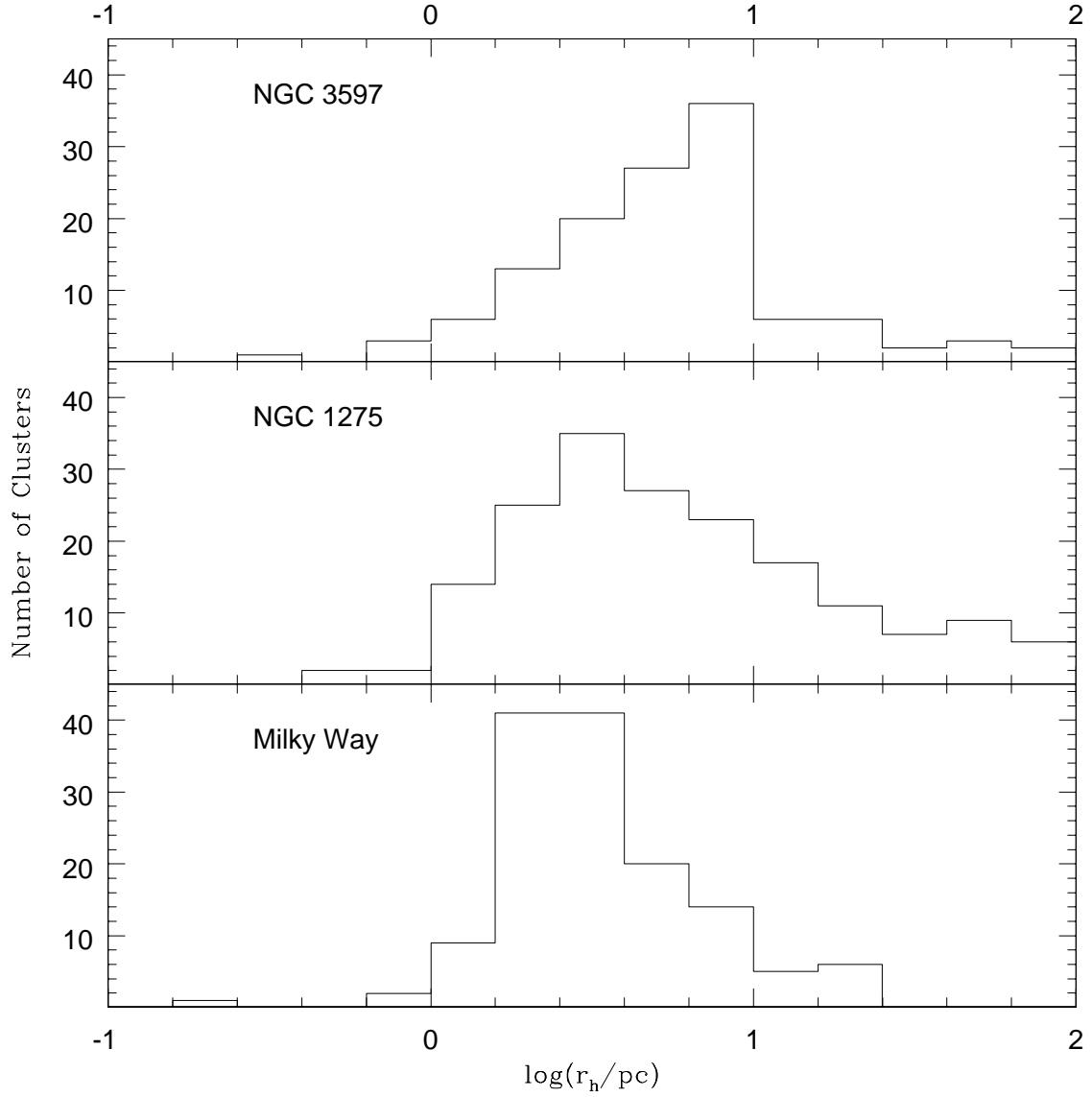


Fig. 16.— Magnitude vs. half-light radius for young clusters in NGC 3597, NGC 1275, and old globulars in the Milky Way. Apparent magnitudes in R for the young clusters and absolute magnitudes in V for old Galactic globulars. Errors on half-light radii are estimated from the simulations based on S/N and do not include possible systematic errors. For the faintest clusters, no error bars are shown since they are fainter than our simulations.

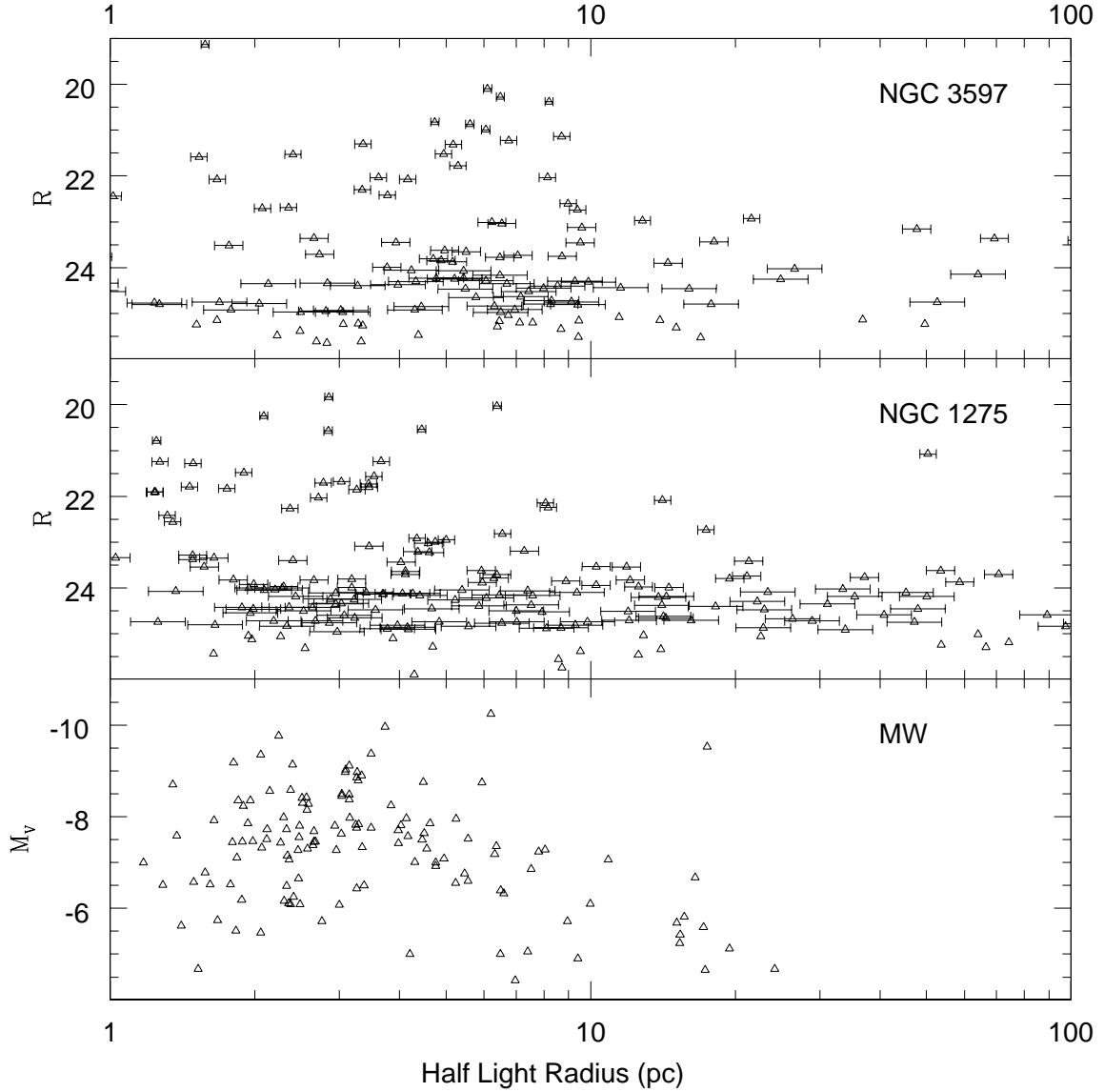


Fig. 17.— Distance from the galaxy center in kpc plotted against half-light radius in pc for NGC 3597, NGC 1275, and the Milky Way. The twenty brightest clusters in the young cluster samples are shown as filled circles. Error bars are as in Figure 16

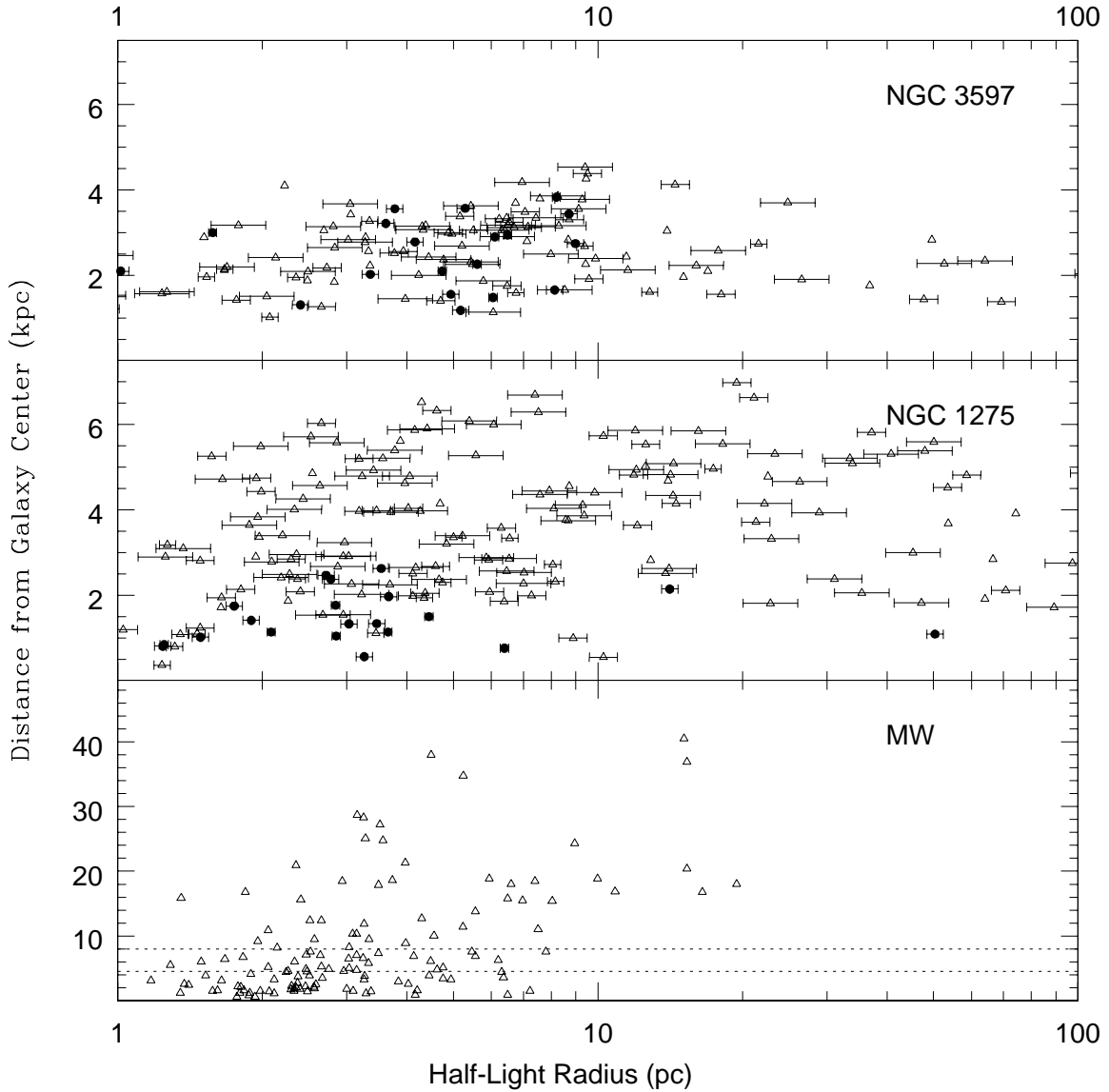


Fig. 18.— Best fit King radius ($c = 2$) vs $m_{0.8} - m_3$ for the 100 brightest clusters in NGC 3597. The 20 brightest clusters in this sample are shown as filled triangles.

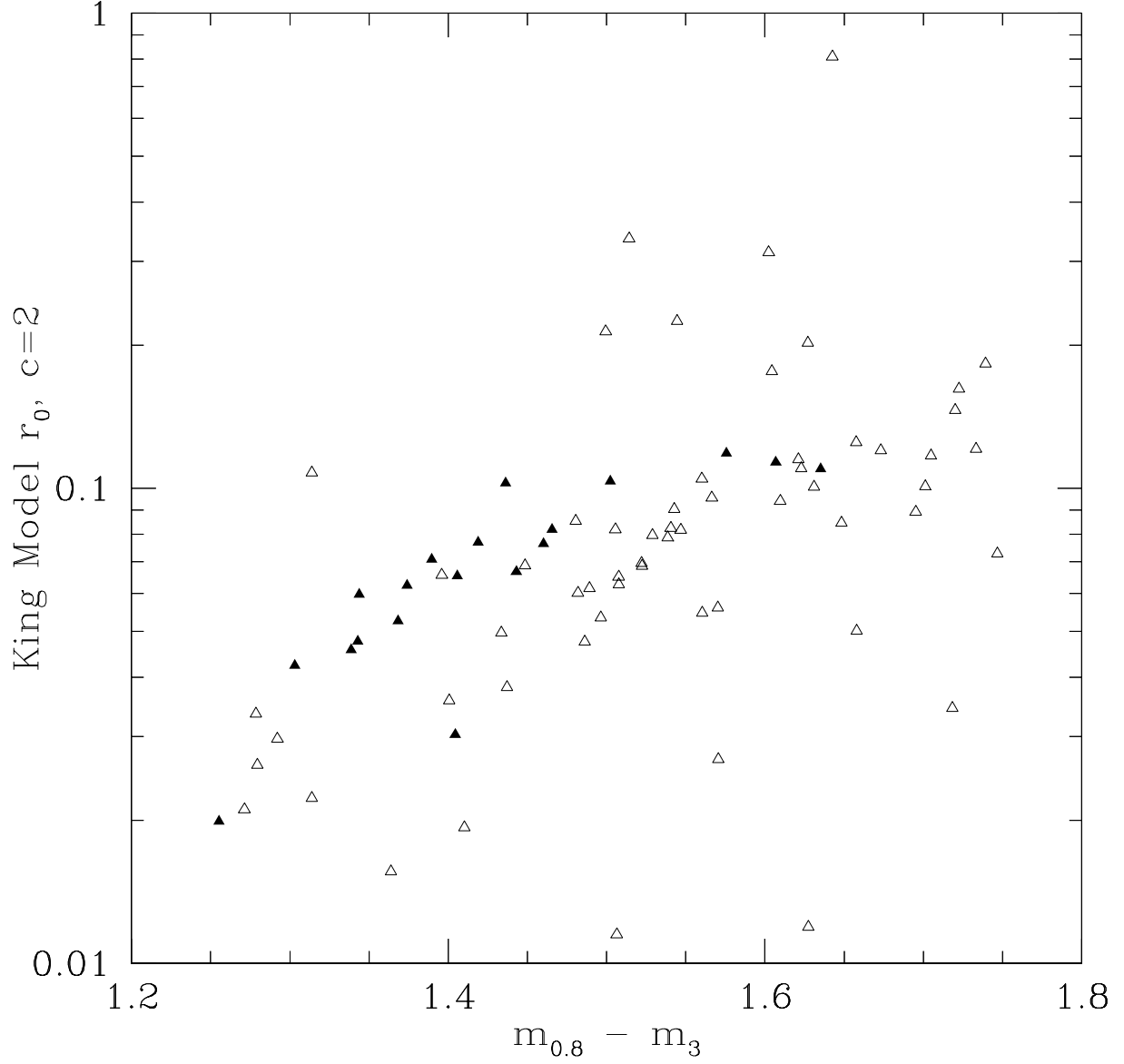


Fig. 19.— Best fit King radius ($c = 2$) vs $\Delta(m_1 - m_2)$ for the 100 brightest clusters in NGC 3597. The 20 brightest clusters in this sample are shown as filled triangles.

